UNITED NATIONS UNIVERSITY
UNU-GTP
Geothermal Training Programme

Orkustofnun, Grensasvegur 9
IS-108 Reykjavik, Iceland

Reports 2019
Number 16

PERFORMANCE STUDY OF A SINGLE-FLASH GEOTHERMAL POWER PLANT COLD END: A CASE STUDY OF OLKARIA II POWER PLANT

Gideon K. Kemboi
Kenya Electricity Generating Company PLC – KenGen
Geothermal Development Division
P.O. Box 785 – 20117
Naivasha
KENYA
gkemboi@kengen.co.ke, gidikkemz@gmail.com

ABSTRACT

The Olkaria II power plant operating conditions of different systems have diverged from the ideal design values over time. The main focus of this study were two systems in the cold end of the geothermal power production process, i.e., the circulating water and the non-condensable gases (NCG) removal systems. The main components studied included the condenser, the cooling tower, NCG removal steam ejectors, inter-condensers and Liquid Ring Vacuum pumps. A comparison study between the original design parameters and the current operating parameters was carried out. The conservation of heat and mass balance throughout the circulation process has been the basis of the analysis. The main operating parameters under investigation are the condenser pressure and circulating water temperatures. The heat load exerted upon the condensers of the three units seems to have risen with an increase in steam consumption. This might have led to an increase of the NCG content in the steam. In addition, the effectiveness of the cooling tower was calculated and found to have deteriorated by almost 20% from the design conditions. The study has taken the maintenance strategies employed on these systems into account with the aim to enhance them. Previous condenser shell punctures and main steam pipe punctures indicated that the corrosive property of the cooling water results from oxidation reactions and a necessity for deaerating. The abundance of oxygen in the cooling water is thought to be a result of the open cooling tower basin and air leakages into the condenser. Eventually most of the focus was on the cooling tower cooling capabilities and the possible factors leading to deterioration in its effectiveness. Fouling has been identified as one of the main causes of deterioration in the performance of the condenser, pipes, cooling tower fills and basin. The chemical dosing process at the power plant has been considered and the sulphur depositions in the cooling water seem to increase with a rise of the pH values. The study compared the design and current parameters but further analysis will be necessary to map out the deterioration trend over time and to improve mitigation strategies.

1. INTRODUCTION

1.1 General background

Olkaria II is a geothermal power plant belonging to the Kenya Electricity Generating Company PLC (KenGen). KenGen currently controls about 75% of the market share of electricity supplied to the consumers in Kenya (KenGen, 2019). Kenya has a diverse power generation mix and the highest quantity by installed capacity are hydro power generation power plants. The national power generation installed capacity in Kenya is currently 2,695 MWe out of which the geothermal power contribution is 690 MWe (Mangi, 2018). An overview of geothermal power plants in Kenya is given in Table 1.

TABLE 1: Overview of installed geothermal capacity in Kenya (Mangi, 2018)

No.	Power plant name	No. of units	Total capacity (MWe)	Type of cycle
1	Olkaria I	3	45	Single flash
2	Olkaria II	3	105	Single flash
3	Olkaria III (Orpower Inc.)	6	155	Binary
4	Olkaria 1 additional units IV&V	2	150	Single flash
5	Olkaria IV	2	150	Single flash
6	Olkaria wellheads	15	81.1	Single flash
7	Oserian	2	2	Binary
8	Eburru wellhead	1	2.4	Single flash
	Total		**690**	

Olkaria V power plant is an ongoing geothermal development project in the Northeastern sector of the Olkaria geothermal field. It is expected to supply an additional 172 MWe by the end of 2019. All the geothermal power plants installed in Kenya are single-flash steam cycles except the units at Olkaria III owned by Orpower Inc. and the Oserian power plant which are binary geothermal systems utilising the Organic Rankine Cycle (Mburu, 2014).

This scenario is attributed to the fact that the Olkaria geothermal field is a high-enthalpy field which is liquid dominated and the temperature ranges between 200 and 340°C in the aquifer (Karingithi, 2000), making it preferably feasible to set up single-flash cycle power plants. A flashing process occurs when the pressurised geothermal fluid changes from liquid to vapour underground due to a reduction in pressure beyond the saturation pressure at a particular temperature (DiPippo, 2012). A single-flash cycle is one where work is done by one flashing process before the fluid is ejected from the system.

Olkaria II (Figure 1) was the second geothermal power plant to be commissioned by KenGen, after Olkaria 1. It comprises 3 single-flash units of 35 MWe each, for a gross electric power output of 105 MWe. The first two units were commissioned in October and November 2003 (Mwangi, 2005) and subsequently a third unit was commissioned in 2010. During the lifetime of the power plant, units 1 and 2 have undergone major overhaul maintenance activities in 2014 and 2012, respectively. Some of the biggest dismantling and replacement jobs during the overhaul involved the turbine and the cooling tower.

The cooling tower fills were found to be quite clogged what significantly impacted the overall cooling system. Combined with constriction of the first stage nozzles of the turbine, this led to a drop of the power plant gross electricity output. The deterioration of the operational parameters has been observed over time and this study seeks to highlight just how much the parameters have deviated from the design conditions. The effect of these deviations will be investigated and also the maintenance strategies that have been adopted to remedy these changes in conditions.

FIGURE 1: Olkaria II power plant aerial depiction, as seen from the Olkaria II view point (Andiva, 2018)

1.2 Location

Olkaria II power plant has been set up within the Olkaria volcanic complex (Figure 2) which is located about 132 km northwest (World Bank, 2010) of the capital city Nairobi. It lies in the rift valley of Kenya in Nakuru county and Naivasha sub-county about 35 km to the southwest of the Naivasha town centre and about 6 km south of the shores of Lake Naivasha within the Hell's gate National Park. This is part of the East African Rift Valley system (EARS) that cuts through several countries from Mozambique in the South to the Red sea in the North of Africa where it intersects the Gulf of Aden at the Afar triple junction (Karingithi, 2000).

Within the Olkaria geothermal complex, the Olkaria II power plant lies in the Olkaria Northeast field (Figure 3) where it is surrounded by other geothermal development facilities, mainly power plants and green houses, with a vast steam gathering system.

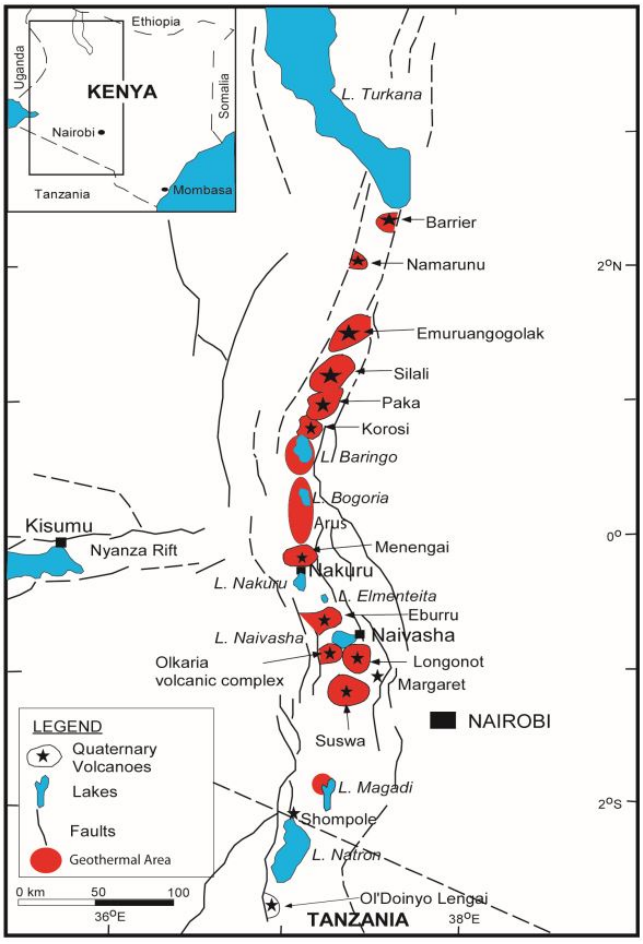

FIGURE 2: Location Of the Olkaria geothermal complex within the eastern branch of the East African Rift System (Muchemi, 1999)

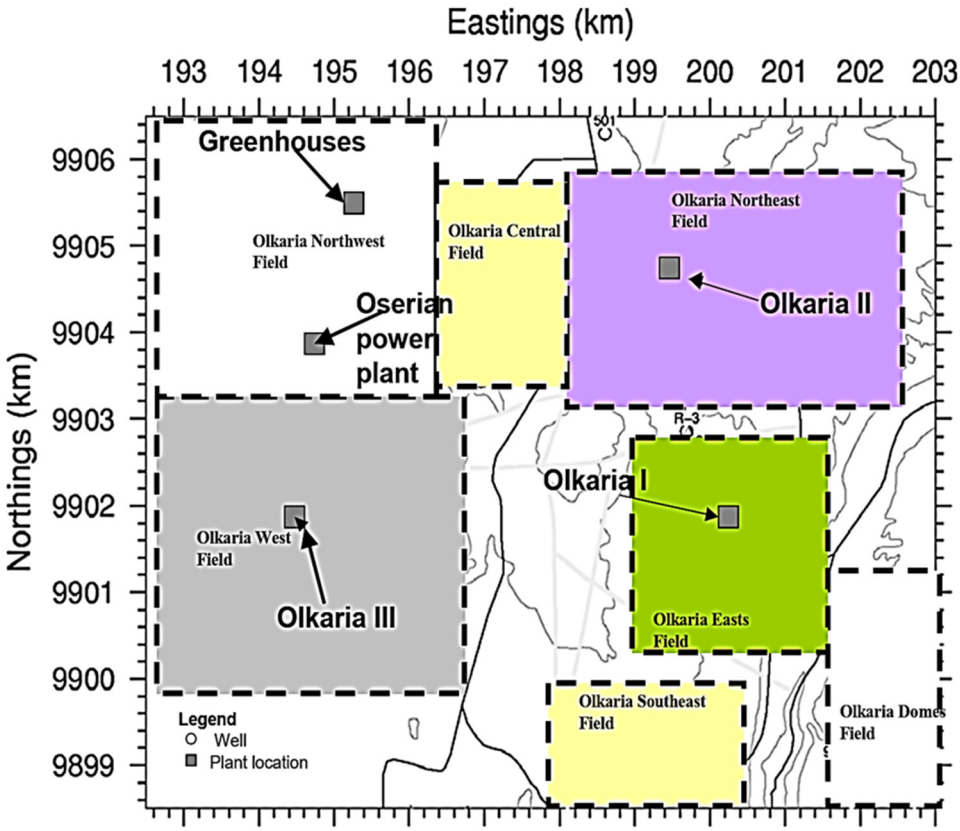

FIGURE 3: Location of Olkaria II power plant within the Greater Olkaria geothermal complex (Mwangi, 2005)

2. OLKARIA II OPERATIONAL STATUS

2.1 Detailed process description

Olkaria II is a single-flash cycle geothermal power plant made up of three similar steam turbine generator units each producing 35 MWe. The geothermal steam is supplied from the Olkaria northeast fields where 22 production wells were drilled between 1985 and 1993 awaiting the power plant construction and additional make-up wells were availed in the year 2000 (Saitet and Kwambai, 2015). The process flow of Olkaria II is shown in Figure 4. The steam is channelled through three main steam pipes, one for each unit. There are several modular water separators located throughout the Olkaria field serving multiple wells before the steam joins the main steam pipe. The brine is separated from the steam and either flows through the silencer to a surface pond or is redirected to a hot reinjection well.

Due to a decline in steam production from the original production wells, some extra wells were connected to the Olkaria II - unit 3 main steam line. The make up steam is drawn from the Olkaria East field and flows through a Pressure Reducing Valve (PRV) to SN3 separator station before it joins the unit 3 main steam line. The three main steam lines then converge to a common vent station and are connected to it through a common header pipe. The common header is connected to the vent station chimneys and the discharge of excessive steam is regulated using 6 vent station valves. These valves operate in a cascade mode to maintain the pressure that is set in the control toom to ensure the required turbine inlet pressure is achieved and any higher steam pressure is discharged or vented to the atmosphere.

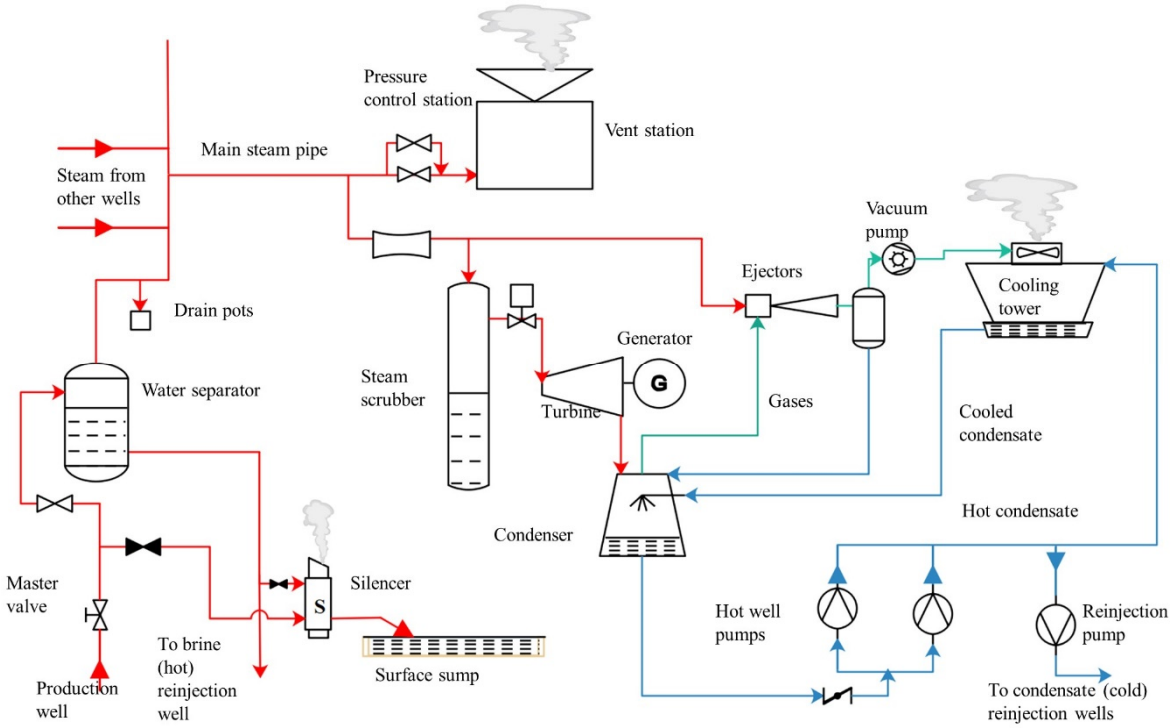

FIGURE 4: Process flow diagram of Olkaria II geothermal power plant

In the event of failure in the vent station valves, resulting in a pressure build up in the steam pipeline, each of the main steam supply lines is fitted with rupture discs. These are 3 pressure step rated rupture diaphragms which will break and release the excessive steam pressure. Upon normalisation of the system, these rupture discs can be manually isolated for replacement without disrupting the power generation process.

The additional steam in the unit 3 pipeline is distributed to units 1 and 2 through inter-connecting loop pipes. The main steam line can be isolated by 3 valves:

1. Remote controlled steam inline valve;
2. Motorised local controlled isolation valve; and
3. Manual wheel operated isolation gate valve.

These valves are normally all closed during major maintenance activities that will require opening of the turbine and condenser access manholes. The inter-connection loops are the point at which the auxiliary steam pipe branches off from the main steam line.

The main steam flows through a Venturi flow meter before reaching the cyclone separator. The flow rate of the main steam supply and the auxiliary steam supply are metered separately. The steam flows into the cyclone separator where condensate that may have formed during steam transportation and solid particles are separated from the steam. This separated water component flows to the flash tank for cooling and disposal to the condensate reinjection pipe or the power plant drains known as the U-seal pit.

After leaving the separator the dry steam flows through a steam pipe that splits into two to allow the steam to flow into the turbine casing from the left hand and right hand sides. Each of these split pipes is fitted with two valves, a Main Stop Valve (MSV) for emergency steam isolation in case of a turbine trip and a Governor Control Valve for real-time regulation of steam flowing into the turbine depending on grid demand and steam pressure. The steam flows through a 6-stage condensing turbine coupled to a generator.

The steam is exhausted downwards into a direct contact condenser after expansion through all stages of the turbine. The condenser has a main cooling water inlet pipe from the cooling tower basin. Smaller vertical pipes branch from this main pipe upwards and have nozzles on their sides which spray jets of cold water onto the incoming steam. This results in condensation of the steam causing a sudden reduction in both volume and pressure inside the condenser shell. The non-condensable gases (NCG) from the condensed steam are sucked out of the condenser by a 2-stage gas extraction system made up of steam ejectors, inter-condensers and a liquid ring vacuum (LRV) pump. The combined effect of the continuous condensation and gas extraction results in a vacuum inside the condenser shell.

The NCG are sucked out of the condenser through a gas cooling chamber where the heat is extracted by the cooling water flowing downwards through a counter flow mechanism before the gases exit the condenser. The gas cooling water is broken down into droplets by perforated horizontal sheets which are stepped inside the gas cooling chamber. The gases are sucked out of the condenser at a first stage by two ejectors, and at a second stage by the LRV pump, a spare ejector, which pumps the gases to atmospheric pressure. The gases are piped to the top of the cooling tower where they are dispersed into the atmosphere by the cooling tower fans.

The condensate and cooling water mixture on the other hand are pumped through risers to the top of the cooling tower by two hot well pumps for cooling. Cooling tower fills are used to increase the interfacial area between the water and the air in order to speed up the rate of cooling (Jackson, 1951). This hot mixture is distributed at the top of the cooling tower by a network of pipes fitted with splash nozzles to spray the condensate over the film fills stack. The film fills form a thin film of water that flows downwards towards the cooling tower basin. This increases the water surface area exposed to the air for cooling. The cold ambient air flows into the sides of the cooling tower and upwards through the fills due to the induced draft by the fans. The counter flow between the air and water is the basis for heat exchange.
The cooling water is drawn from the cooling tower basin by the condenser vacuum and the auxiliary cooling water pumps through a fibre reinforced plastic (FRP) pipe. The component cooling water pumps supply the cooling water to the generator air coolers, lube oil coolers, flash tank and the inter-condensers of the NCG extraction system. The discharged water from the generator and lube oil coolers flows directly to the cooling tower basin. However, the inter-condensers discharge their cooling water into the condenser where it mixes with the condensate for subsequent pumping by the hot well pumps.

The water in the cooling tower is subjected to chemical treatment for pH and microbiological growth control. The cooling tower make-up water is obtained from the condensate of the incoming steam. The water level in the cooling tower level is automatically regulated by periodic starting and stopping of the reinjection pumps to maintain the level within a pre-defined range.

2.2 Circulating water and NCG removal systems set up

The two main types of condensers used in a single-flash geothermal cycle are the direct contact condenser and the surface contact condenser. The condensers utilised at Olkaria II are down exhaust direct contact jet condensers with an adjoining cascade tray type gas cooling chamber. The design properties of each jet condenser for the three units are shown in Table 2 (MHI, 2010).

The cooling tower is made up of 4 cells per unit. The fans are driven by fixed speed horizontal electric motors rated at 150 kW and coupled to a fibre reinforced shaft. The rotation axis is translated from horizontal to vertical using a gear reducer. The cooling tower fan blades are kept at a scooping angle of 20°. The volume of air flowing through the fans is therefore expected to be constant.

TABLE 2: Main properties of the condensers installed at Olkaria II for all three units

No.	Properties	Value
1	Vacuum pressure	0.075 bar-abs
2	Cooling water inlet temperatures	21.3°C
3	Cooling water flow rate	7900 m^3/h
4	Spray nozzles diameter	50 mm
5	Gas cooler trays holes diameter	3 mm
6	Empty weight	80 tons
7	Operational weight	157 tons
8	Water filled weight	410 tons

The NCG system at Olkaria II comprises 2 stages (Figure 5). The first stage is made up of a set of 3 ejectors each with a corresponding inter-condenser. The ejectors operation mode is 3×50%. Therefore, two ejectors are always in service while the third ejector is kept on stand-by. The second stage is made up of a LRV pump with a 1×100% configuration and a back-up ejector with an after condenser also with a 1×100% configuration.

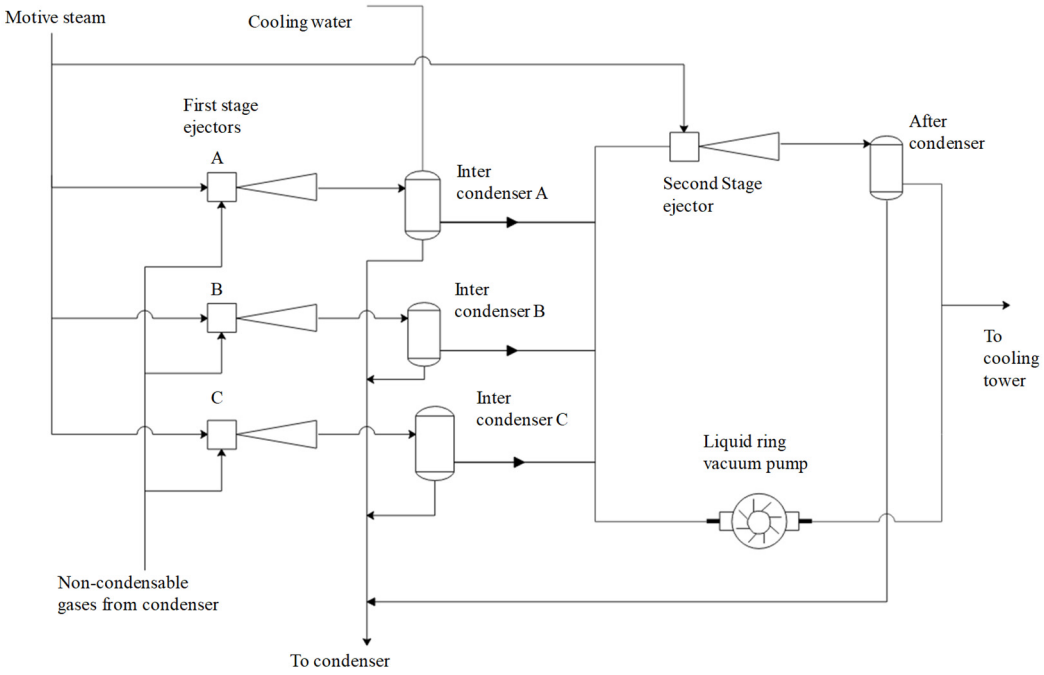

FIGURE 5: Simple flow diagram of the NCG extraction system at Olkaria II

The LRV pump runs alone during normal operation and the back-up ejector automatically starts in the event of tripping of the pump. Usually the main reason for tripping of the LRV pump is a rise in the suction temperature of the gas from the gas ejectors. Due to the poor vacuum condition, the second stage of gas removal often sees the LRV pump and the backup ejectors running together. This results in higher steam consumption and cooling water requirements.

2.3 Design and current parameters

From the detailed process description in the previous section, the cold end of the process begins once the steam has been fully expanded and is exhausted from the low-pressure end of the turbine. This means the main systems under consideration are the circulating water system and the NCG extraction system. The main components of the circulating water system are the condenser, hot well pumps and the cooling

tower. On the other hand, the NCG extraction system mainly comprises of the ejectors, LRVP, inter-condenser and after-condenser.

This study compares the design conditions of the power plant to the current operating parameters. The current operation parameters have been obtained from a randomly sampled control room parameters log sheet manually filled in by the operators for 30th July 2019 when all the units were in running condition Appendix I. The design parameters to be used in the study were compiled from the Olkaria II power plant hand book and systems manuals prepared by the power plant main contractor Mitsubishi Heavy Industries (MHI, 2003a) which are also the original equipment manufacturers of the turbine and generator (Appendix I).

3. DESCRIPTION OF WORK

3.1 Analysis data

The performance analysis was done by making a comparison between the design conditions as stated in the systems manuals and the current operating conditions from the control room log sheets filled in at Olkaria II power plant by the operators. For the current parameters, the values used were an average of 5–6 readings captured in the log sheets during the day and night shifts. Table 3 shows a compilation of the main parameters under consideration in this analysis of both the design conditions and the sampled current conditions.

TABLE 3: Design and current operating parameters at Olkaria II power plant

No.	Parameter	Units	Design units 1 & 2	Design unit 3	Current Unit 1	Current Unit 2	Current Unit 3
1	Steam mass flow rate	T/h	252.45	253.90	270.00	268.02	285.70
2	Steam mass flow rate	kg/s	70.13	70.53	75.00	74.45	79.36
3	Separation pressure (vent station)	bar-a	5.00	5.00	6.14	6.17	6.14
4	Turbine inlet pressure	bar-a	4.80	4.80	5.81	5.87	5.86
5	Turbine inlet temperature	°C	150.30	150.30	154.82	157.72	157.41
6	Condensation temperature (hot well water temperature)	°C	40.30	40.30	50.96	51.44	52.34
7	CT inlet water temperature	°C	37.30	37.30	51.24	53.96	52.24
8	CT discharge water temperature	°C	21.30	21.30	19.08	34.72	31.54
9	Condenser vacuum pressure	bar-a	0.075	0.075	0.144	0.169	0.143
10	Power output	kW	34,830	35,140	33,080	35,280	35,620

The readings are normally recorded by the operator at tentative intervals of 4 hours. An assumption has been made that the recorded data at the control room is from reliable measurement equipment but in case the parameter variation from the expected value is too high, a possible problem with the measurement equipment has been considered.

The design parameters of units 1 and 2 are similar. However, they vary slightly from those of unit 3 which was installed about 8 years after the former units. The parameters chosen for analysis are those that are continuously recorded during the operations process. A good proportion of the other ambient conditions that are not recorded regularly will be assumed to have not changed over time.

The design parameters used in Table 3 are at 100% nominal capacity rating (NCR) conditions from the heat and mass balance (HMB) diagrams of each unit (MHI, 2003a). The mass flow rate of the steam is only for the motive steam flowing into the turbine excluding the auxiliary steam consumption. This is because the main steam line and the auxiliary steam lines have separate Venturi-flow meters. Assumptions made in the data compilation are:

- The values recorded were from reliable monitoring and measurement equipment;
- The ambient conditions have remained largely the same since the design period, i.e., the relative humidity, dry and wet bulb temperature, humidity ratios, atmospheric pressure and more; and
- The value of atmospheric pressure is 0.8 bar absolute. This is the value to be added to any gauge pressure readings during data analysis.

The relationship between the different forms of pressure representations are shown in Figure 6. All the pressure values displayed on the Operator stations (OPS) of the distributed control system (DCS) at Olkaria II are gauge pressure (bar-g) values. The exceptions are the vacuum pressure and the ejector pressures which are given in absolute pressure (bar-a).

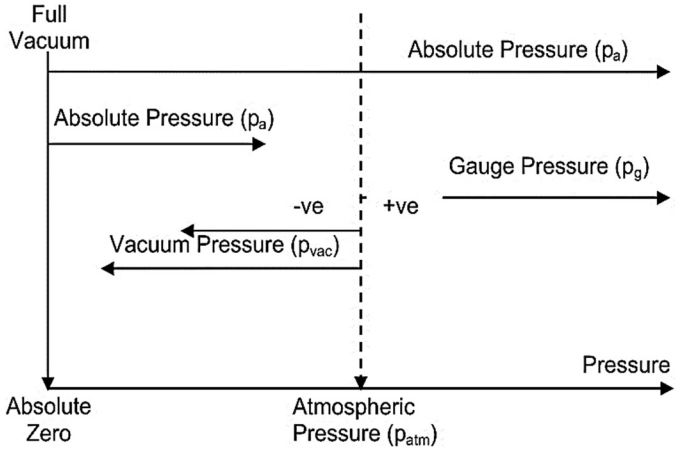

FIGURE 6: Representation of the relationship between atmospheric pressure, gauge pressure and absolute pressure (Edwards and Otterson, 2014)

Therefore, the gauge pressure readings of the current operating conditions have to be converted to absolute pressure readings for uniformity during analysis. This is done by addition of the atmospheric pressure value to the gauge pressure values as shown in Equation 1 (Edwards and Otterson, 2014):

$$bara = barg + Atmospheric\ pressure \quad (1)$$

The condenser pressure is already expressed in absolute pressure. It is important to ensure that the condenser pressure remains low to:

1. Increase the output of the turbine;
2. Raise the overall efficiency of the power plant; and
3. Reduce the steam consumption of the power plant.

However, there are several reasons that may limit the formation and sustenance of the condenser vacuum. The factors expected to affect the condenser back pressure are as follows (Bhoi et al, 2015):

1. Variation in design cleanliness factor with load;
2. Amount of latent heat to be removed – a function of both generator load, (i.e., exhaust flow rate) and condenser backpressure;
3. Cooling water inlet temperature;
4. Cooling water flow rate – number of C.W. pumps operating and/or extent of tube sheet fouling;
5. Degree of fouling of the condenser tubes;
6. Concentration of non-condensables which have accumulated in the condenser shell or, alternatively, the amount of air in-leakage into the system; and
7. Performance of air removal system.

All these factors except the first two which are design dependent can be mitigated through appropriate maintenance activities.

NCG. The main factor to consider in the gas extraction system adoption is the quantity of the non-condensable gases contained in the steam supply (Millachine, 2011). There are three main types of equipment that can be used for NCG removal:

1. Steam ejectors;
2. Compressors; and
3. Liquid ring vacuum pumps.

The presence of NCG in the steam has no negative impact on the turbine performance until the condensation process takes place in the condenser. The quantity of NCG in the Olkaria II main steam supply is about 0.75% by weight (Ndege, 2006). When the condensable portion of the steam is condensed they shrink in volume and only the NCG remain occupying the same volume. These gases will accumulate in the absence of an appropriate gas removal system resulting in back pressure from the turbine.

3.2 Computational analysis

The design data was used to prepare an EES model of the design conditions (Appendix II). The parameters of interest could then be varied to see what would be the expected effect on the rest of the system parameters. The single-flash process diagram shown in Figure 7 was used as the basis for the analysis model with the energy flow shown in the T-s diagram in Figure 8. The current operating parameters were then input into the code to establish the expected change both in the power output and the isentropic efficiency assuming the power plant units are still operating at or close to full load (Appendix II).

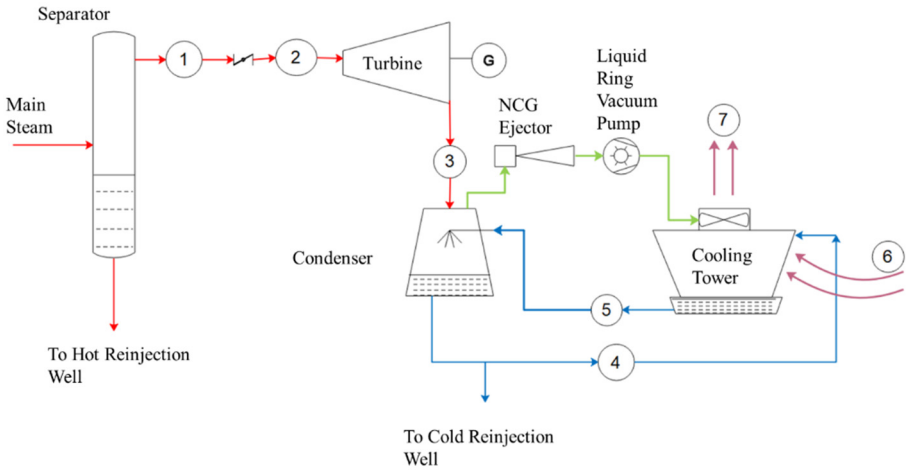

FIGURE 7: Single-flash process flow diagram

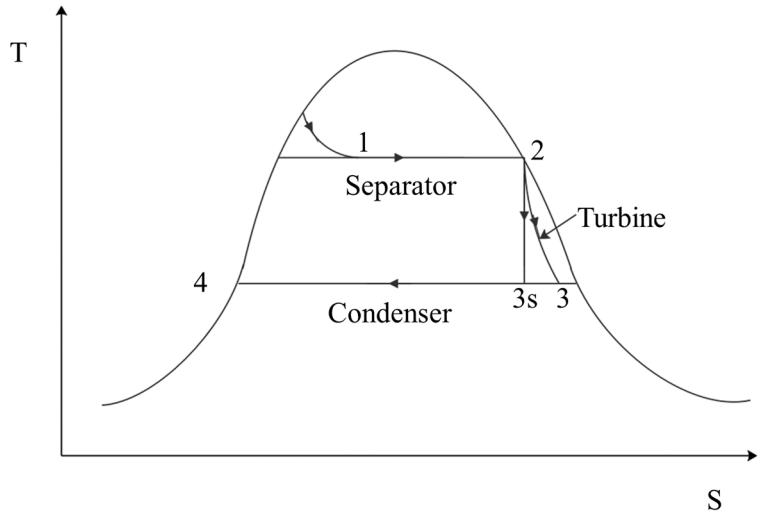

FIGURE 8: T-s diagram of single-flash power plant

For a mechanical draft cooling tower, the main performance evaluation data required for thermal testing are the water flow, the water temperatures at inlet and outlet, the wet bulb temperature and the fan horsepower (Hensley, 2006). A specific experimental thermal test was not conducted, thus the data used was extracted from the manuals and operating conditions log sheets. The first step was identification of the independent parameters that would be used as inputs in the process flow diagram. The identified independent variables were:

1. Turbine inlet steam mass flow rate (after separator);
2. Turbine inlet steam pressure;
3. Condenser vacuum pressure;

4. Cooling tower inlet water temperature;
5. Cooling tower outlet water temperature; and
6. Power output.

The initial conditions were considered to start at the turbine inlet, thus disregarding the reservoir conditions and separation pressure drops during the computational analysis. The inlet steam pressure, enthalpy and steam quality values were the fixed variables used to calculate the properties at different stages of the single-flash cycle. Once the main steam had expanded through the turbine, the isentropic efficiency ($\eta_{isentropic}$) was established using the design enthalpy conditions in Equation 2 (DiPippo, 2012):

$$\eta_{isentropic} = \frac{h_2 - h_3}{h_2 - h_{3s}} \tag{2}$$

The turbine isentropic efficiency is the ratio of the actual work done to the work done at a constant entropy. The isentropic efficiency considering the design parameters was found to be $\eta_{isentropic} \approx 0.80$ for all three units with unit 3 being slightly higher.

Condenser

After the last stage of the turbine, the steam is exhausted downwards into the direct contact condenser. The cooling water flowing into the condenser is sprayed onto the exhaust steam extracting latent heat from it causing the steam to condensate. The steam volume suddenly shrinks due to this change of state resulting in the formation of a vacuum in the condenser.

To analyse the cooling process, it is essential to first find out the heat load that has been subjected to the condenser from the turbine exhaust. This heat load will affect the efficiency of the cooling tower since it is ideally equal to the amount of heat that is extracted by the cooling tower. The condenser heat load is given by Equation 3. Considering conservation of energy, the total heat and mass flow of the condensate leaving the condenser is given as the sum of the heat and mass flow of the incoming cooling water and the condensed steam:

$$\dot{m}_4 h_4 = \dot{m}_3 h_3 + \dot{m}_5 h_5 \tag{3}$$

The condensate from each unit is pumped out of the condenser by two 400 kW hot well pumps running at a configuration of 2×100% to the top of the cooling tower.

Cooling tower

The cooling tower should be designed to be able to handle the heat load of the steam that is exhausted from the turbine into the condenser. The type of cooling tower at Olkaria II power plant is a mechanical induced draught counter flow cooling tower (Figure 9). There are different numerical methods that can be used to analyse cooling tower performance. In a numerical study undertaken on a counter flow wet cooling tower, it was found that the heat lost through evaporation at the top of the cooling tower packing was 90% compared to only 65.2% at the bottom (Khan et al., 2003). The results are however method dependent.

The mechanical draught counter flow cooling tower design is based on the total-heat theory developed by Merkel in 1925 (Jackson, 1951). According to this theory, the overall cooling effect is a result of cooling due to loss of latent heat at the water surface and sensible heat from the main water body being cooled.

Considering the counter flow between the rising air and the falling water droplets, the heat exchange process involves an exchange of both heat and mass between the air and the water. According to the first law of thermodynamics or conservation of energy, the rate of heat loss by the water at a constant mass flow rate is expected to be similar to the heat gained by the air at constant flow rate. Therefore, the total heat lost by the water to the air Q is described by Equation 4:

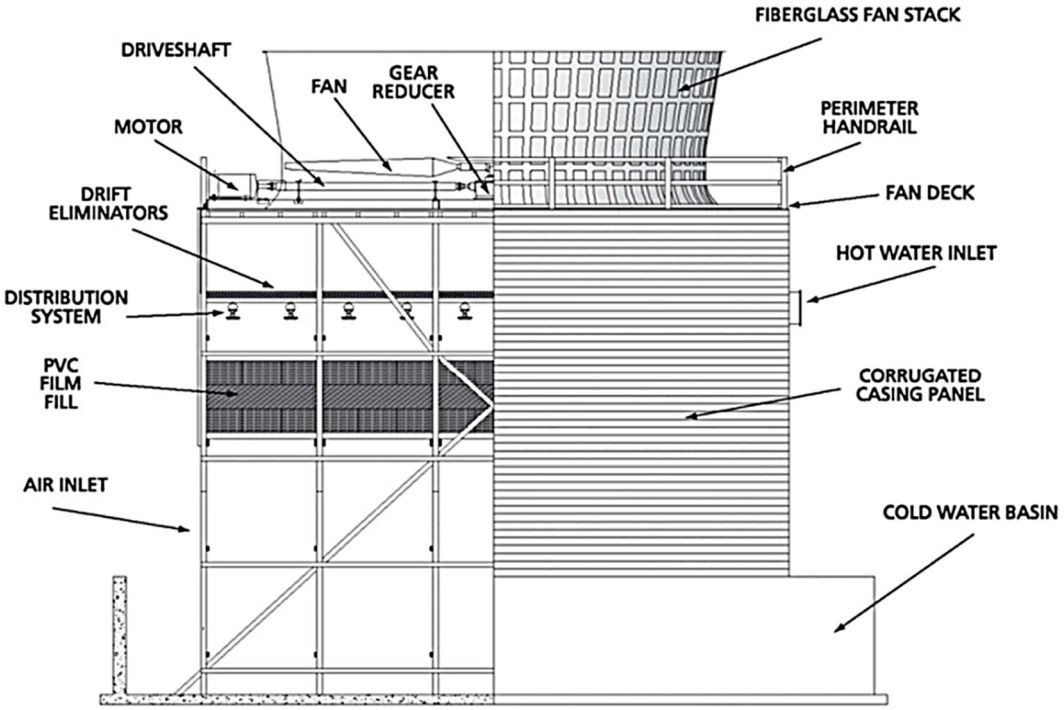

FIGURE 9: Partial cut away section of a mechanical induced draft counter flow cooling tower cell (Verkís, 2019)

$$Q = \dot{m} C_p (T_4 - T_5) \tag{4}$$

where $\dot{m}$ = Mass flow rate of water (kg/s);
C_p = Specific heat capacity of water (kJ/kg/°C);
T_4 = Cooling tower inlet water temperature (°C); and
T_5 = Cooling tower exit water temperature (°C).

On the other hand, the maximum heat that can be extracted by the air from the water Q_a is obtained as follows:

$$Q_a = \dot{m}_a (H_{a2} - H_{a1}) \tag{5}$$

where Q_a = Maximum heat flow in air (kJ/kg);
$\dot{m}_a$ = Mass flow rate of the air (kg/s);
H_{a2} = Total heat or enthalpy of the exit air (kJ/kg); and
H_{a1} = Total heat or enthalpy of the inlet air (kJ/kg).

Assuming no other heat losses, the rate of cooling is therefore given by Equation 6 (Jackson, 1951):

$$\dot{m} C_p (T_4 - T_5) = \dot{m}_a (H_{a6} - H_{a7}) \tag{6}$$

The heat and mass balance in this case is as follows:

$$h_4 \dot{m}_4 + h_6 \dot{m}_6 + h_{a6} \dot{m}_{a6} = h_5 \dot{m}_5 + h_7 \dot{m}_7 + h_{a7} \dot{m}_{a7} \tag{7}$$

For purposes of this study the numbers denoting the different points of the cycle are as presented in Figure 7. The parameters for water are denoted by numbers in the subscript only, while the parameters for air have an ‘a’ in the subscript preceding the number. The relative humidity in the air is given as a ratio of the partial saturation and saturation pressures of air.

This therefore means that for any cooling tower design the following parameters must be known beforehand:

1. Flow rate of the water to be cooled;
2. The range of temperatures through which the cooling will take place; and
3. The wet bulb temperature of the air.

In Equation 7 it is assumed that the mass flow rate of water $\dot{m}$ remains unchanged throughout, meaning that losses to evaporation are considered negligible. The efficiency of the cooling tower $\eta_{coolingtower}$ can then be determined by the ratio of the actual cooling and the maximum possible cooling that can take place with reference to the wet bulb temperature T_{wb}. Computation of the efficiency will consider range and approach which are defined as follows (Figure 10):

- *Range:* This is the temperature difference between the water flowing into the cooling tower for cooling and the temperature of the discharged water.
- *Approach:* This is the temperature difference between the cooling tower discharge water (cold) and the lowest possible temperature that can be achieved.

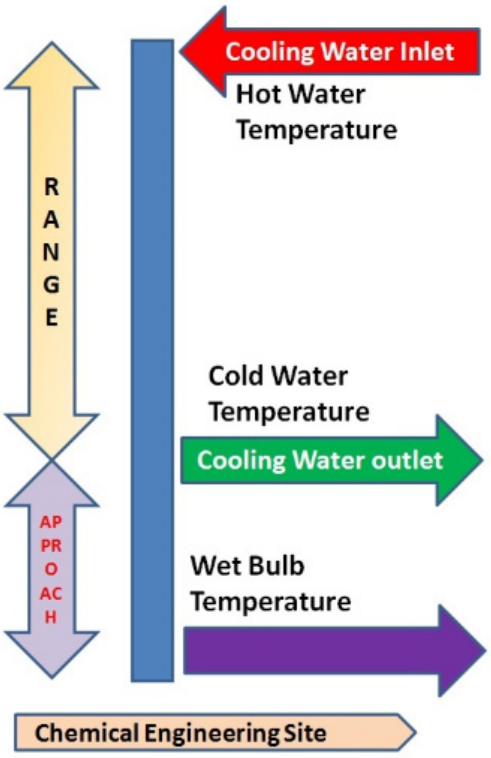

FIGURE 10: Simple graphical representation of range and approach of a cooling tower (Chemical Engineering, 2019)

The lowest possible temperature achievable is the ambient wet bulb temperature. The cooling tower efficiency is therefore given by the following relationship between the range and approach:

$$CT\ Efficiency = \frac{Range}{Range + Approach} \times 100 \tag{8}$$

To find the maximum possible cooling that can take place, the range and approach values are summed up. The lowest achievable temperature is the wet bulb temperature. Therefore, the cooling tower efficiency is given by Equation 9:

$$\eta_{coolingtower} = \frac{T_4 - T_5}{(T_4 - T_5) + (T_5 - T_{wb})} \tag{9}$$

Considering the design conditions from the heat and mass balance diagram, a brief EES analysis model was established starting at the point of separated steam ending at the turbine power output.

The condensate is available as make up water for the cooling tower basin since it is an open loop system which is susceptible to evaporation losses unlike steam supplied by boilers. However, in the Olkaria II design the condensate reinjection pumps are triggered by level switches at the cooling tower basin to run periodically and not continuously. This ensures that the water level inside the cooling tower remains stable at an operational height of about 1.85 m (MHI, 2010). Assumptions:

1. Air leaving the cooling tower is saturated with water vapour (relative humidity = 1 or 100%);
2. Steady flow of both air and water;
3. Adiabatic conditions;
4. No loss of mass due to blowdown;
5. The mass flow of dry air into the tower is the same as the mass flowing out;
6. The ambient conditions have remained the same since the design period; and
7. The volume flow rate out of the cooling tower fans is constant.

The conservation of mass and energy is considered in the cooling cycle. Mass flow of water is given by the following equation:

$$\dot{m}_4 + \dot{m}_6 = \dot{m}_5 + \dot{m}_7 \quad (10)$$

The mass flow of dry air considering assumption 5 is as follows:

$$\dot{m}_{a6} = \dot{m}_{a7} \quad (11)$$

However, properties of wet air (air H_2O) are used in the calculation of the heat exchange in the EES analysis model to compute the properties of the air before and after cooling the water. Considering these balances, the performance of the system was calculated by checking the change in values of the turbine efficiency, the condenser heat load and the cooling tower efficiency (Appendix III).

Gas ejectors and liquid ring vacuum pumps
The computational analysis focused on the cooling system involving the condenser and the cooling tower. Therefore, in the analysis model the parameters of the ejectors and liquid ring vacuum pump are excluded. The extent of the gas extraction was one of the challenges encountered during the operation and maintenance activities.

3.3 Operation and maintenance strategies

3.3.1 Condenser

The condenser does not undergo any routine maintenance during operation. Preventive inspection and maintenance activities are scheduled annually. The main maintenance activities undertaken inside the condenser is the cleaning of the gas cooling chamber trays and inspection of the condenser shell for potential leakage. However, periodic emergency shut downs have been occasioned by perforations on the condenser wall. The resulting effect is leakage of air into the condenser during operation or water flowing out of the condenser once the vacuum is eliminated or in the case that the perforation is below the water level.

FIGURE 11: Gas cooler trays clogged by elemental sulphur

During the annual inspections, the staggered perforated sheets in the gas cooling chamber have been found to be almost completely clogged with elemental sulphur (Figure 11). During operation, the cooling water flows into the top of the gas cooling chamber to allow for counter flow cooling of the gases as they are sucked out. However, once the perforations on the sheets get clogged the water accumulates on the sheets instead of flowing through as water droplets.

The result is a reduction in heat exchange between the cooling water and the NCG which contributes to a slight rise in temperature inside the condenser vessel. In addition, the impact of water spilling over from the upper trays and the weight of the accumulated water causes the clogged perforated sheets to break (Figure 12). A gaping hole is left behind which allows the water to flow down in a single stream without being broken down into droplets. The broken pieces will then be found on the next level or on the condenser floor during the scheduled maintenance.

Cooling water chemistry and chemical dosing

The reason for chemical treatment of the circulating water system ranges from the prevention of scaling and biological slime formation to pH control. According to a cooling water chemistry and dosing analysis report prepared by Sinclair Knight Merz (SKM, 2011), there were several findings in the Olkaria II cooling tower fouling. The study was carried out after unit 3 had been in operation for one year. The chemical additive at the power plant is mainly for pH control. An alkaline 5% soda ash solution (Na_2CO_3), prepared from 95% pure Magadi soda ash, is injected into the condensate at various points.

FIGURE 12: Gas cooler trays broken due to the weight of accumulated cooling water

The pH of the condensate formed in the condenser ranges from 2 to 3 before chemical treatment. The soda ash solution is expected to raise the pH of the condensate flowing to the cooling tower to between 4.5 and 5.5 and the pH of the water flowing to the cold reinjection wells to between 6 and 8 (MHI, 2003b). This is done by pumps supplying the chemical solution to the hot well discharge pipe and another set of pumps supplying the solution to the blow down pipe. Both sets of pumps are reciprocating pumps.

During the study, an observation was made on the cooling tower basin water as shown in Figure 13. When chemical treatment was ongoing, the water in the cooling tower seemed to be continuously cloudy. While without the treatment the cooling tower basin water was clear. This led to the suspicion that the dosing process was actually an encouraging factor to depositions in the circulating water circuit.

FIGURE 13: Left: Cooling water in the Olkaria II basin during dosing;
Right: When no dosing is taking place (SKM, 2011)

According to the study, deposition of sulphur was highest in the condenser especially below the water level where the deposition thickness ranged between 1 and 5 mm and thinned out towards the cooling tower where the study found only a thin film of deposited sulphur. In addition to that, a sample of the cooling tower sludge was tested and the sulphur composition in it was found to be over 90%. This sulphur deposition is expected to be a result of oxidation reactions by the H_2S in the condensate. The path of this reaction is described by the chemical Equations 12, 13 and 14 (Bacon et al., 1995):

$$2H_2S + 2O_2 = H_2S_2O_3 + H_2O \quad (12)$$

$$5S_2O_3^{2-} + 4O_2 + H_2O = 5SO_4^{2-} + H_2SO_4 + 4S \quad (13)$$

$$4S + 6O_2 + H_2O = 4H_2SO_4 \quad (14)$$

These equations show that the oxidation of H_2S results in the formation of elemental sulphur S and sulphuric acid H_2SO_4. Without chemical dosing, the circulating cooling water would continuously be acidic at a pH of 2–3. The effect of this low pH has been felt in the main steam supply pipes which have been punctured following sessions of blade washing or de-superheating using the condensate.

From Figure 14, the formation of sulphates and the formation of elemental sulphur deposits seemed to be greater when dosing rates were increased as shown by the increase in sodium ions concentration. This is because a rise in pH towards a neutral pH creates a favourable environment for the formation and existence of more sulphates (Finnbogi Óskarsson, personal communication). The sodium ions in the solution do not react further with any elements in the condensate, so they do not have any chemical implication on the sulphur deposition.

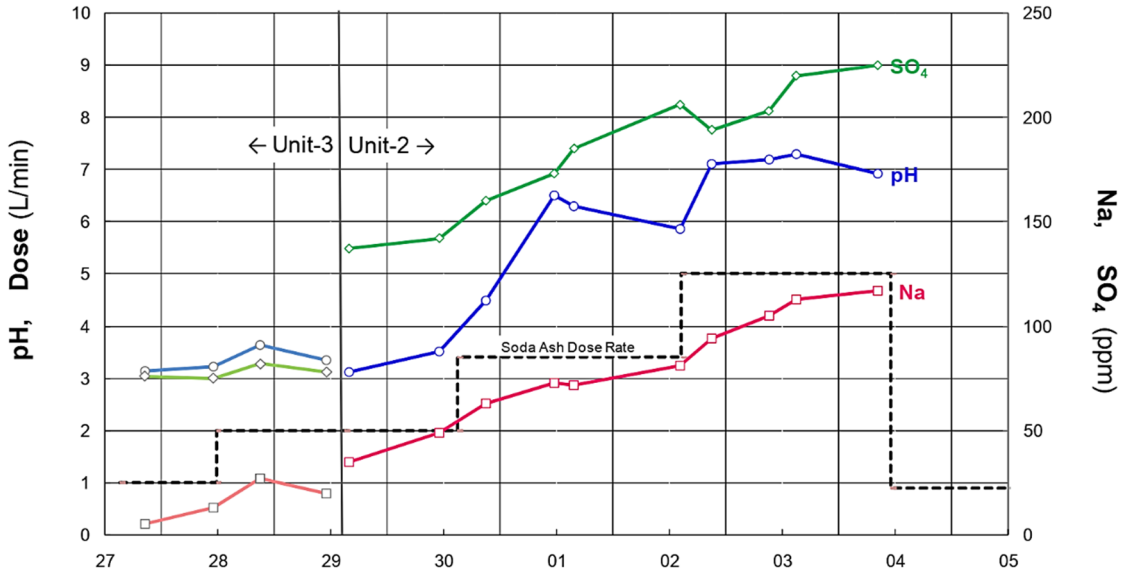

FIGURE 14: Demonstration of increase of sulphates with increase of sodium content in the cooling water as observed between June 27 and July 4, 2011 (SKM, 2011)

A higher concentration of sulphates results in increased deposition of elemental sulphur due to the oxidation reactions in the condensate and cooling water mixture. Since the cooling tower basin is open, there is abundant oxygen getting into the water during the evaporative cooling process. Therefore, the oxygen content in the cooling water cannot be regulated, meaning the sulphates concentration is the limiting factor in the oxidation reactions. A balance needs to be established for an optimum pH level of the cooling water that reduces sulphur deposition and corrosion of equipment.

3.3.2 Cooling tower

The cooling tower is made up of a wide range of components as seen earlier in Figure 9. Therefore, multiple maintenance strategies have to be employed to cover them all:

- Oil change for the cooling tower fans' gear boxes is scheduled after a total of 2,490 running hours for units 1 and 2 and 2,990 running hours for unit 3.
- Condition based maintenance triggered by equipment trips and high temperatures or vibrations include:
  - gearbox replacement (bearing failure, oil seizing as grease and shearing of gears); and
  - replacement of fan blades occasioned by high vibrations due to breaking off of the plastic blades end caps.

Scheduled maintenance activities include annual inspection and major overhauls. Annual inspection and maintenance of the cooling towers involves the following processes:

- Removal of condensate distribution pipes and nozzles for cleaning of sulphur deposits;
- Repair of ripped/broken partitioning walls; and
- Draining of the water from the cooling tower basin and removal of the accumulated sludge from the bottom of the basin.

A major overhaul was carried out 8 years after commissioning and every 5 years since following the OEM recommendation. The activities carried out are largely similar to those carried out in the annual inspection. Additionally, all the cooling tower film fills (Figure 15) have to be removed and replaced with new ones.

FIGURE 15: Cooling tower fills removed during unit 1 overhaul maintenance in July 2014

Over time, gradual fouling of the cooling tower fills occurs due to growth of microbial organisms and the accumulation of solidified elements from the condensate. This necessitates periodic replacement of the fills to maintain their ability to form a thin water film to increase the cooling surface area. Figure 16 shows the debris that had accumulated in a section of the cooling tower fills and Figure 17 shows the accumulation of elemental sulphur in the cooling tower main distribution pipe. Several pieces of the fills broke off during the maintenance process most likely owing to the weight of the sediments in the fills and pooling of the incoming water. The replacement of the fills was the most laborious task in the cooling tower overhaul program but critical to the restoration of the cooling tower efficiency.

FIGURE 16: Debris that had accumulated in the cooling tower film fills before the major overhaul

The improvement in the cooling tower performance after the maintenance has not been quantified. This requires reference to the log sheets that were filled in tentatively a week or two before the units were shut down for major maintenance. The main cooling tower water

FIGURE 17: Accumulated sulphur deposits in the common header of the distribution pipes

distribution pipe has a lot of sulphur deposits. These deposits eventually end up in the smaller distribution pipes and onto the splash nozzles.

3.3.3 Ejectors and LRV pump

The NCG removal system main components are the steam ejectors, inter-condensers, and the LRV pump. Each unit has 3 ejectors and inter-condensers on the first stage of gas removal, 2 in service and 1 backup. Due to the backup ejector in both the first and second stages of the gas extraction system, the components may block or stick due to long periods of non-use. To remedy this, one of the operation strategies implemented in the first stage of the NCG removal system is periodic rotation of the service and backup ejectors as shown in Table 4.

TABLE 4: Sample rotation schedule of the first stage ejectors

Week no.	Ejector A	Ejector B	Ejector C
1	In service	In service	Standby
2	In service	Standby	In service
3	Standby	In service	In service
4	In service	In service	Standby

The first stage ejectors are labelled A, B and C as seen earlier in Figure 4. The rotation cycle should be weekly. The rotation schedule minimises the mentioned problems and at the same time enables periodic monitoring of the ejectors' performance. This routine will enable the operator to identify a faulty ejector depending on the effect that it has on the condenser vacuum pressure. The changeover process requires adjustment of a manual steam supply throttling valve to achieve the best possible vacuum conditions. The valve should then remain in this position even when changeover has taken place until the next exchange. The adjustment to the optimum steam flow position is a hectic process and dependent on the feel and experience of the operator.

The main problem encountered with the ejectors is leakage of the ejector steam and gas isolation valves of the standby ejector. Steam isolation valve leakage manifests in two forms:

1. Back flow of steam into the NCG common header and back to the condenser; and
2. Flow of steam into the NCG discharge pipe through the inter-condenser to the LRV pump.

The first scenario is experienced if the steam leakage is coupled with the NCG isolation valve leakage. This directly contributes to a deterioration in the condenser vacuum pressure by introduction of a back pressure. The remedy for this is to put the ejector in service and to set the ejector with good sealing properties to standby. This will effectively disrupt the weekly change over schedule until corrective maintenance is carried out on the leaking valves.

The second scenario results in a rise of the discharge temperature of the NCG after the first stage. This temperature rise results in tripping of the LRV pump due to the inlet temperature which exceeds the interlock value of 50°C (MHI, 2003a). The LRV pump trip is the trigger for the second stage back up ejector to automatically start running. This is counteracted by allowing the cooling water to flow into the standby inter-condenser to prevent the steam from reaching the NCG discharge line. However, the rise in temperature of the gas flowing to the LRV pump in the second scenario may not necessarily be the result of a leakage. It could be a normal result of high condenser pressure and high cooling water temperature. Remedial action in this case is to redirect the cooling water to the cooling tower.

Considering that no major inspection or repairs can be done on the ejectors and its valves during operation, an annual inspection is scheduled. This inspection can be antedated in case of a breakdown of another equipment part that requires a long downtime period.

The annual inspection program of the steam ejectors involves removal of a flange spacer to examine the ejector mouth for clogging and depositions (Figure 18). The isolation valve wheels are also serviced to ensure that the gears are in good working condition. In the event that a leakage is suspected during operation, the valve is removed and inspected. Any deposition is remedied by facing of the deposited material or greasing of the pins.

FIGURE 18: Ejector opened during annual inspection in 2016

The LRV pump inspection and maintenance also takes place annually. The annual inspection mainly entails inspection of the coupling, oil change of the gear box and greasing of the bearings.

4. RESULTS AND DISCUSSION

4.1 Process models' comparison

Thermal testing of a cooling tower is the only accurate way to determine its actual performance level when in operation (Hensley, 2006). A model of the operating conditions was created using the computational analysis described in Section 3.2. The modelled design conditions for units 1 and 2 are similar (Figure 19), while a few of the parameters vary slightly for unit 3 but are largely similar (Figure 20). These design models were prepared using the design data obtained from the system manuals. They form the baseline for a comparison to establish how much the current parameters differ.

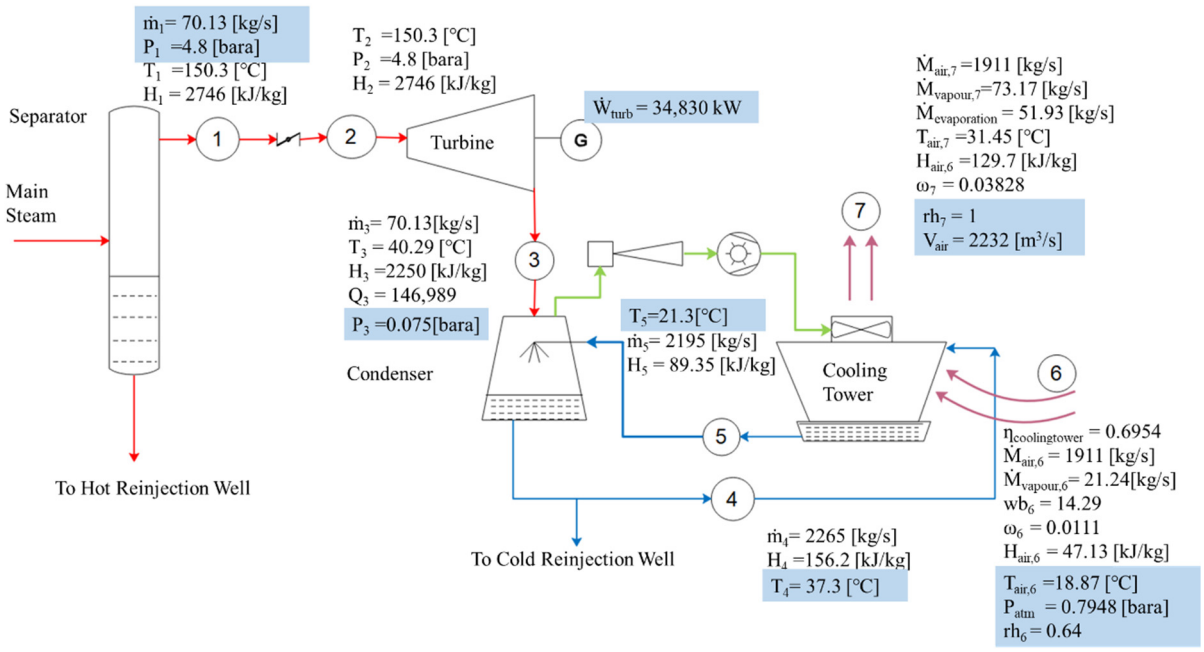

FIGURE 19: Design conditions analysis model for units 1 and 2 in 2016

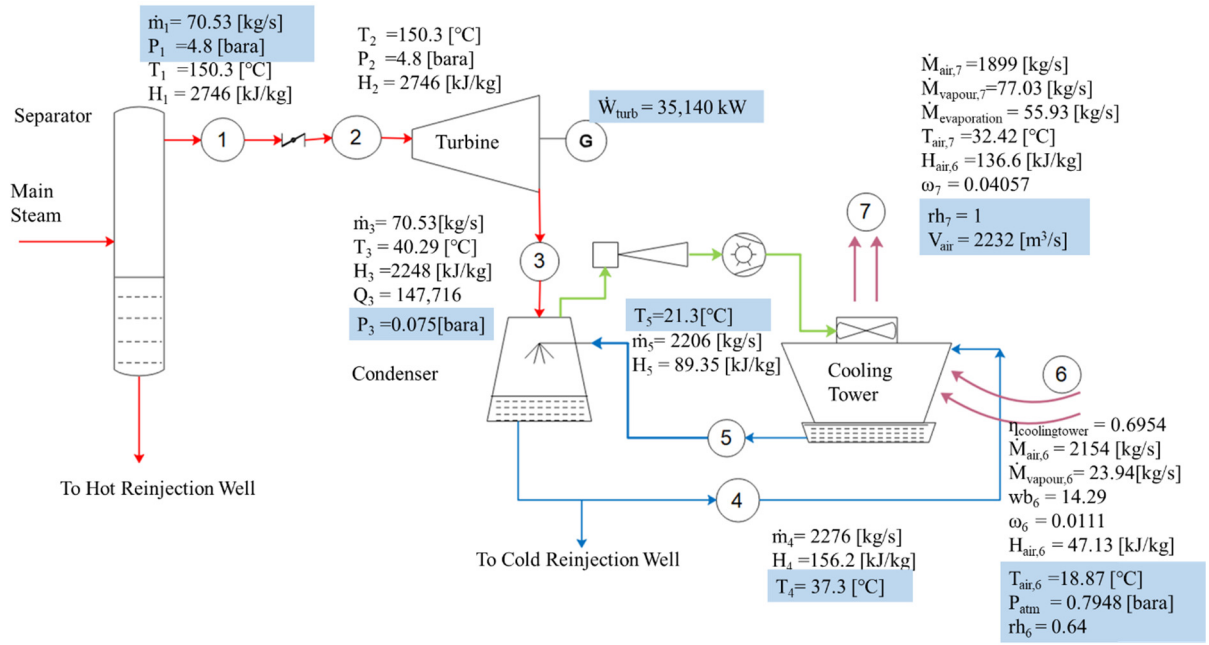

FIGURE 20: Design conditions analysis model for unit 3

The main parameter differences between the design models of the former and latter units are:

1. The main steam mass flow rate; and
2. The power output at 100% nominal capacity rating.

Not included in the model but observable from the heat mass balance diagrams is the auxiliary consumption. The steam consumption values for units 1 and 2 and for unit 3 are 7,592 kg/hr and 6,140 kg/hr, respectively. The current parameters were also put in the models for units 2 and 3 (Figures 21 and 22). The modelling was only carried out for unit 2 and 3 because the unit 1 cooling tower water discharge temperature value was unrealistically low at 19°C.

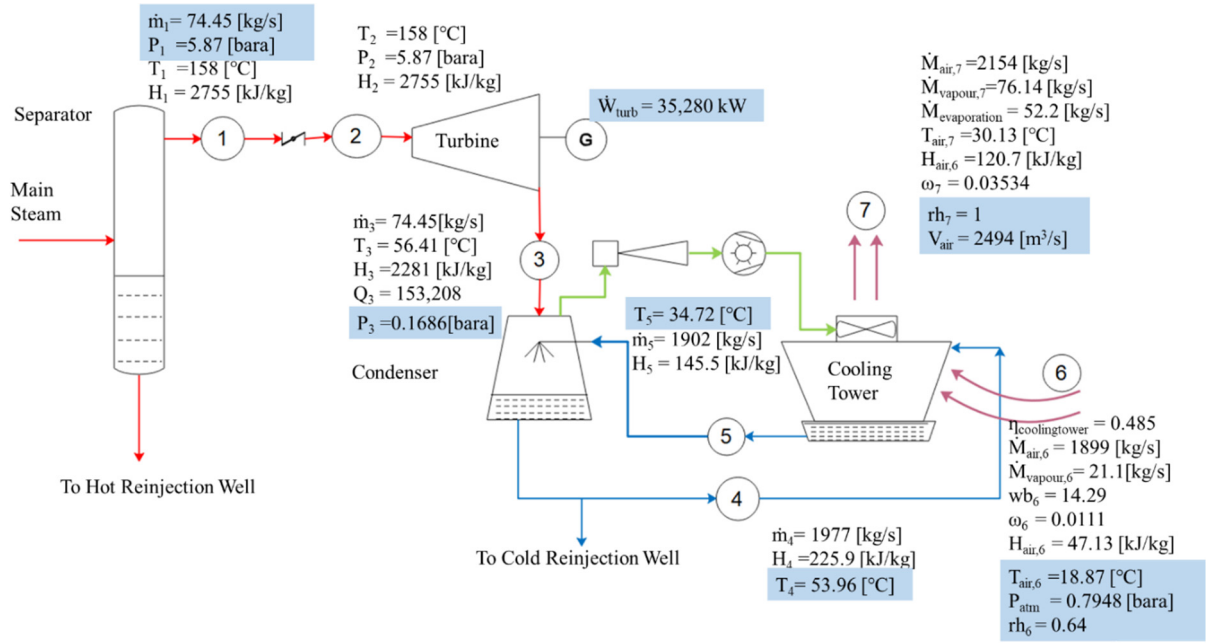

FIGURE 21: Current operating parameters model for unit 2

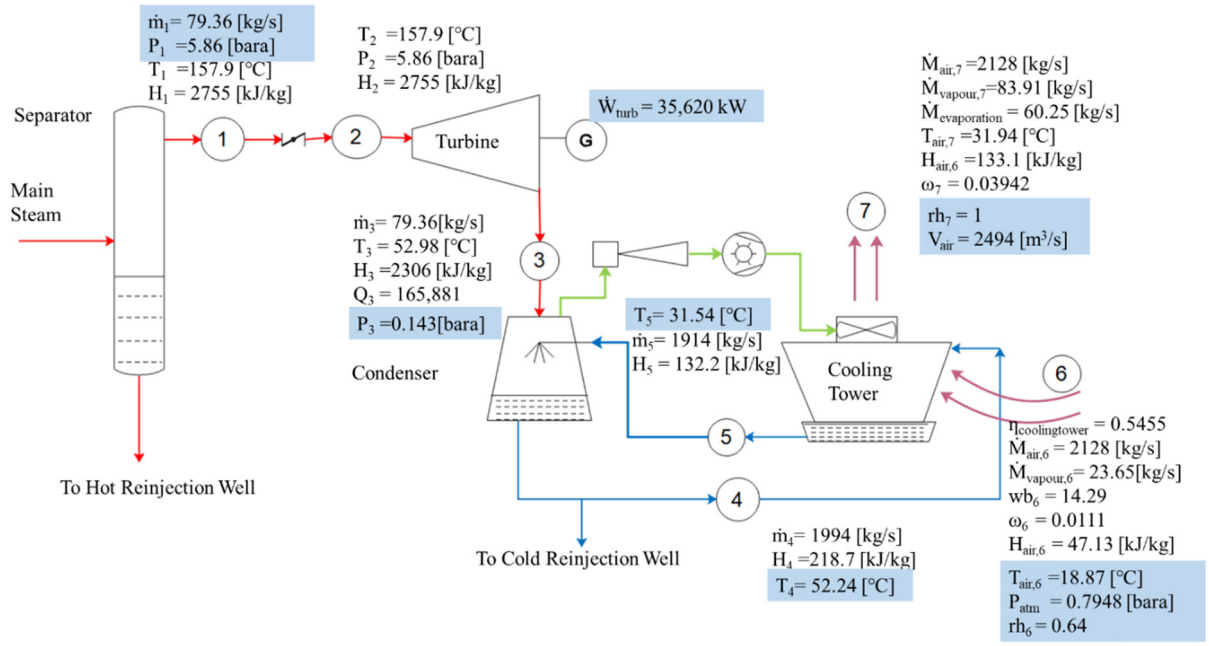

FIGURE 22: Current operating parameters model for unit 3

Upon insertion of the current operating parameters into the unit 2 analysis model, it was noticed that there was a rise in the turbine isentropic efficiency from 0.8062 to 0.8647. This was a red flag considering that the current turbine efficiency cannot possibly be much higher than the design efficiency. The comparison shows that the main steam consumption in unit 2 seems to have risen by almost 4 kg/s while the turbine inlet pressure is now higher by a little over 1 bar. On the other hand, the unit 3 steam mass flow rate seems to have risen by over 9 kg/s. The operating pressure in this case has similarly risen by a little over 1 bar.

Table 5 shows a direct comparison of the design and current parameters of units 2 and 3. The comparison shows that the isentropic efficiency of unit 2 has gone up by close to 6% while for unit 3 it has dropped by about 2%. The rise of the isentropic efficiency in unit 2 cannot be correct after 16 years of operation and 6 years after the first major overhaul in August 2012. Unit 3 on the other hand has been running for 9 years without any major overhaul activities. The drop in efficiency by 2% is expected.

TABLE 5: Comparative study of isentropic efficiency changes with mass flow rate and pressure

No.	Parameter	Unit 2			Unit 3		
		Design	Current	Difference	Design	Current	Difference
1	Steam flow rate (kg/s)	70.13	74.45	4.32	70.53	79.36	8.83
2	Turbine inlet pressure (bar-a)	4.8	5.87	1.07	4.8	5.86	1.06
3	Isentropic efficiency (%)	80.62	86.47	5.85	80.88	78.97	-1.91
4	Condenser heat load (kJ/kg)	146,989	153,208	6,219	147,719	165,881	18,162
5	Cooling tower efficiency (%)	69.54	48.50	-21.04	69.54	54.55	-14.99

The comparison indicates that the input values of unit 2 are not correct. The steam flow rate is expected to have risen much more than its current level as is the case in unit 3. A possible explanation could be that the steam flow measurement equipment in unit 2 is faulty or out of calibration. Therefore, a study of the parameter changes in unit 3 may be more representative of the true turbine condition.

The change in heat load compared to the design conditions (Table 5) is also significantly higher in unit 3 than unit 2. This rise in heat load is one contributing factor to the high operating temperature of the condenser. This is expected due to a higher steam consumption rate in both units. Condenser back

pressure is a direct result of the turbine performance. The turbine performance is affected by the pressure levels in the condenser where the steam is exhausted (Bhoi et al., 2015). The operation of the turbine becomes less economical when the heat rate rises.

The calculated cooling tower efficiency values have dropped in unit 2 and 3 by about 21% and 15%, respectively. A similar efficiency calculation could not be performed for unit 1 because its cooling tower discharge temperature of 19°C was unrealistically low. The cooling tower efficiency and condenser heat load seem to have an inverse relationship. The results obtained from Equation 9 only consider the heat losses but not the electrical components.

The cooling tower efficiency calculation however does not tell the full story about the operating conditions. The design cooling range spans over 16°C (21.3–37.3°C) for both units 2 and 3. The current operating conditions cooling range is about 19°C for unit 2 (34.72–53.96°C) and 21°C for unit 3 (31.54–52.24°C). The cooling range is much higher in the current conditions. However, due to the high approach values, the efficiency drops significantly due to the increase in the denominator value of Equation 9.

The effect of this high temperature at the cooling tower outlet, which is about 13°C higher than the design value, is a compromised heat exchange in both the main condenser and the inter-condensers of the gas extraction system. Coupled with the increased heat load exerted on the condensers of both units, the cooling water jets will condense the exhaust steam from the turbine at a much slower rate. Since steam is being admitted at a higher pressure and the cooling rate is reduced, the uncondensed steam with the NCG will cause a rise in the condenser vacuum pressure. Therefore, the temperature of the condensate cooling water mixture that is pumped out of the condenser to the cooling tower is about 16°C higher than the expected design value of 37.3°C.

The flow rate of the cooling water is reduced compared to the design operation parameters. This is a result of high vacuum pressure in the condenser. The head of the flow is reduced since the condenser pressure is much closer to the atmospheric pressure of 0.8 bara. Therefore, there will be less suction force of the cooling water exerted by the condenser from the cooling tower. This will in turn further encourage a rise in temperature in the condenser.

FIGURE 23: A jet of water flowing out of a hole in the unit 2 condenser shell in 2018 at the top of the cooling tower

Air leakage into the condenser is another suspected cause of the rise in condenser pressure reducing the turbine efficiency due to an increase in back pressure. Figure 23 is an example of one of the perforations detected in the condenser wall as seen during the hydro test. The perforations or points of leakage may not be easy to detect but depending on the magnitude the effect will be observed due to deterioration of the vacuum. The inspection procedure currently involves momentary filling of the condenser shell with water once the vacuum has been broken.

The trade-off of the LRV pump tripping and the starting of the second stage ejector is a reduction in auxiliary power consumption and an increase in the auxiliary steam consumption. However, due to deterioration of the vacuum conditions, both systems run concurrently.

4.2 Mitigation

The maintenance strategy implemented for the ejectors should be taken a step further to include borescope inspection. This will enable monitoring of the deposition at the ejector - pipe interface and not just at the mouth or ejector inlet. Although the deposition on the ejector walls is not expected to be as high as on the turbine first stage nozzles.

The cooling water pH should be analysed to establish the optimum pH at which elemental sulphur formation from oxidation and corrosion is reduced. Elemental sulphur cannot be cleared without shutting down the unit and draining the pipes and cooling tower basin. When depositions have formed on the cooling tower film fills the only solution is replacement. A redundancy in the cooling towers is a drastic measure which can be considered to minimise downtime for fills replacement.

The condenser does not require a lot of maintenance activities. Monitoring of the oxygen content in the extracted NCG allows an estimation of the amount of air leakage into the condenser. This can be a starting point to inspect the condenser shell for possible leakages that would add up to the measured air quantity. The broken gas cooler trays have been replaced with thicker perforated sheets with bigger diameter holes than the original sheets which had 3 mm diameter holes. This modification results in water droplets that are much bigger and thus a lower surface area is exposed to the NCG for heat exchange. The trade-off is a lower likelihood of clogging by elemental sulphur and handling of more water weight and impact without breaking.

Challenges
Most of the available historical data is preserved on hard copy log sheets and a longer-term performance trend needs a much longer study period to allow for digital data entry. The reason for this manual maintenance of logs is a breakdown in the storage module of the DCS system which was restored in January 2019. The study was limited to design and current operating conditions since the historical data was held in hard copy during the study period and it would have required a longer period for compilation and analysis.

Due to operation at high condenser pressure, a breakdown in 1 of the 4 fans per unit results in a drop in power output. This is mainly experienced in units 1 and 2. Trying to maintain a full load when one cooling tower cell is not functional would result in operation of the vacuum unloader. Unit 3, however, has a more robust design. The full power capacity of 35 MWe can be produced with 3 out of 4 cooling tower cells running but with a decline in vacuum conditions.

5. CONCLUSIONS AND RECOMMENDATIONS

The performance analysis of the circulating water system and the gas extraction system has shown a decline in the efficiency of the cooling systems. Considering the data being monitored by the control room operators, more attention was given to the cooling tower which is responsible for the bulk heat extraction. The main issue affecting the cooling tower performance seems to be fouling by both elemental sulphur and microbial growth. This has resulted in a 14–20% decline in cooling tower performance.

The condenser also contains sulphur deposition but the two main factors influencing its performance are increased heat load on all units and air leakages. The clogging and breaking off of the gas cooling trays would result in reduced cooling of the NCG exiting the condenser but the effect on the condenser vacuum and temperature should be minimal. It will however have an impact on ensuring that the NCG temperatures do not rise to the trip level of the LRV pump.

The air leakage into the condenser seems to be a result of perforations in the condenser shell. Some of the leakages are at the condenser shell – concrete interface at the bottom and are possibly a result of

stagnant water at the interface creating favourable conditions for corrosion. Gas sampling of the NCG exiting the condenser should be adopted to check for oxygen availability. Considering that there is no oxygen in the incoming steam, the quantity of oxygen in the extracted NCG should indicate the extent of air leakage into the condenser.

From the findings of the SKM research, the chemical dosing regimen seems to encourage the formation of sulphur deposits in the cooling tower basin. The soda ash solution is the most appropriate alkaline for the chemical dosing. Alternatives would be sodium or potassium hydroxide but these are strong alkaline solutions in comparison. The hydroxide solution would require much more care in handling than the soda ash solution and storing large quantities of it would be hazardous.

The recorded data from unit 3 and subsequent findings were considered to be a better representation of the actual parameters in comparison to the earlier units 1 and 2. However, all three units require inspection and calibration of monitoring equipment to confirm that the parameters shown are the actual values or within their acceptable tolerance. Calibration of measurement equipment may not affect the daily operation of the power plant as long as the values maintain a constant trend. However, the same values would be misleading in case of troubleshooting or when used for scientific analysis that requires the actual values.

Due to the effect of fouling on the cooling tower fills, a more frequent film fills replacement programme should be considered rather than awaiting the overhaul period. However, in case a chemical solution can be found for online dissolution of deposited sulphur, the film fills replacement programme may be avoided. The condenser air leakage should be quantified by measurement of the NCG content flowing into the turbine and the air-NCG ratio flowing out of the gas extraction system.

Further studies will be necessary to quantify the performance of the gas extraction system. However, bore scope inspections should be adopted for the ejectors for a more thorough inspection of depositions without dismantling. The circulating water system performance analysis undertaken was a one on one comparison of the design and current parameters of Olkaria II power plant. A longer-term study is required to establish a trend of the performance deterioration of the cooling tower and condenser and to evaluate the improvement after major maintenance or overhaul activities. This will involve compilation of hard copy data over the units' operation period.

ACKNOWLEDGEMENTS

I would like to express my sincere gratitude to the government of Iceland, the United Nations University Geothermal Training Programme (UNU-GTP) and my employer, Kenya Electricity Generating Company – KenGen, for granting me the opportunity to attend this training programme. I owe my sincere appreciation to Mr. Lúdvík S. Georgsson, the director of UNU-GTP. I would also like to thank my supervisors Thorleikur Jóhannesson and Davíd Örn Benediktsson from Verkís Consulting Engineers for their guidance, support, insight and advice during my project period. I have surely broadened my perspective. I appreciate the help from my colleagues at Olkaria II power plant for heeding my call for technical assistance.

Many thanks to Mr. Ingimar Haraldsson, Dr. Vigdís Hardardóttir, Mrs. Málfrídur Ómarsdóttir, Mr. Markús A.G. Wilde and Ms. Thórhildur Ísberg for their assistance during the travel preparations and my stay in Iceland.

I especially thank and owe heartfelt gratitude to my wife Rosemary Kemboi for her endurance and constant encouragement throughout this period and I want to mention particularly my son Kenan. I sincerely appreciate my family members and friends for their unwavering support, encouragement and patience throughout my absence for the six months. To God be the glory for this far that I have come.

NOMENCLATURE

HMB	= Heat mass balance;
NCG	= Non-condensable gases;
ORC	= Organic Rankine cycle;
LRV pump	= Liquid ring vacuum pump;
Q	= Heat (kJ/kg);
$\dot{m}$	= Mass flow rate of water (kg/s);
$\eta_{isentropic}$	= Isentropic efficiency;
T	= Temperature (°C);
h	= Enthalpy (kJ/kg); and
C_p	= Specific heat capacity of water (kJ/kg/°C).

REFERENCES

Andiva, Y., 2018: *Kenya to start construction of 70 MW geothermal power plant in the Olkaria.* Construction Review Online, article, Group Africa Publishing Ltd, website (September 6th 2018): *www.constructionreviewonline.com/2018/09/kenya-to-start-construction-of-70mw-geother mal-power-plant-in-the-olkaria/*

Bacon, L., Jordan J., and Pearson W., 1995: Microbiology and corrosion in geothermal natural draft cooling towers. *Proceedings of the World Geothermal Congress 1995, Florence, Italy*, 2387-2389.

Bhoi, R., Mehta N., Bhojak K., 2015: Effect of condenser backpressure on power plant heat rate and thermal efficiency. *International J. Scientific Research & Development, 3-3*, 2 pp.

Chemical Engineering, 2019: *Cooling tower efficiency calculations.* Chemical Engineering, article updated in 2018, website*: www.chemicalengineeringsite.in/cooling-tower-efficiency-calculations/*

DiPippo, R., 2012: *Geothermal power plants: Principles, applications, case studies and environmental impact* (3rd ed.). Butterworth - Heineman, Elsevier, Kidlington, UK, 600 pp.

Edwards, J.E., and Otterson, D.W., 2014: Tech talk: (4) Pressure measurement basics. Themed paper in: *J. Measurement and Control, 47-8,* 241–245.

Hensley, J.C., 2006: *Cooling tower fundamentals* (2nd ed.). Marley SPX Cooling Technologies Inc, Overland Park, KS, 117 pp.

Jackson, J., 1951: *Cooling towers with special reference to mechanical draught systems.* Butterworths Scientific Publ. and Imperial Chemical Industries Ltd., London, 104 pp.

Karingithi, C.W., 2000: Geochemical characteristics of the Greater Olkaria geothermal field, Kenya. Report 9 in: *Geothermal training in Iceland 2000.* UNU-GTP, Iceland, 165-188.

KenGen, 2019: *About us*. Kenya Electricity Generating Company - KenGen, Kenya, website: *www.kengen.co.ke/index.php/our-company/who-we-are.html*

Khan, J., Yagub, M., and Zubair, S.M., 2003: Performance characteristics of counter flow wet cooling towers. *Energy Conversion and Management, 44-13*, 2073-2091.

Mangi, P.M., 2018: Geothermal development in Kenya: Country updates. *Paper presented at Sustainable Development Goals Short Course III on Exploration and Development of Geothermal Resources organized by UNU-GTP and KenGen, Naivasha, Kenya,* 33 pp.

Mburu M., 2014: Geothermal energy utilization at Oserian flower farm – Naivasha. *Paper Presented at Short Course VI on Utilization of Low- and Medium-Enthalpy Geothermal Resources and Financial Aspects of Utilization", organized by UNU-GTP and LaGeo, Santa Tecla, El Salvador,* 6 pp.

MHI, 2003a: *Olkaria II plant handbook.* Mitsubishi Heavy Industries & KenGen, 322 pp.

MHI, 2003b: *Olkaria II maintenance manual, system 10: chemical injection system.* Mitsubishi Heavy Industries & KenGen, 300 pp.

MHI, 2010: *Olkaria II maintenance manual, system 5*. Mitsubishi Heavy Industries & KenGen, 871 pp.

Millachine, M.A.T., 2011: *Guidelines for optimum gas extraction system selection.* University of Iceland, Reykjavik, MSc thesis, 54 pp.

Muchemi, G.G., 1999: *Conceptualised model of the Olkaria geothermal field*. The Kenya Electricity Generating Company, Ltd., internal report, 46 pp.

Mwangi, M., 2005: Country update report for Kenya 2000-2005. *Proceedings of the World Geothermal Congress 2005, Antalya, Turkey,* 3 pp.

Ndege, J.W., 2006: Maintenance challenges in the operation of a geothermal power station: a case for Olkaria II plant – Kenya. Report 14 in: *Geothermal training in Iceland 2006*. UNU-GTP, Iceland, 261-290.

Saitet, D., and Kwambai, C., 2015: Wellhead generating plants: KenGen experience. *Proceedings of the World Geothermal Congress 2015, Melbourne, Australia,* 6 pp.

SKM, 2011*: Olkaria II cooling water chemistry report*. Sinclair Knight Merz, unpublished report, contracted by KenGen for the analysis, New Market, Auckland, 36 pp.

Verkís, 2019: *Cooling towers.* Verkís, unpubl. lecture presentation at the University of Iceland, 50 pp.

World Bank, 2010: *Olkaria II geothermal expansion project*. World Bank, project design document for CDM activities, version 8, 61 pp.

APPENDIX I: Randomly sampled control room parameters log sheet and design parameters from the Olkaria II power plant hand book and systems manuals

			DAYSHIFT						Date	30.07.19		
		UNIT-1			UNIT-2			UNIT-3			[i]
ITEM DESCRIPTION	UNITS	800	1200	1600	800	1200	1600	800	1200	1600	REMARKS
UNIT LOAD	MW	33.2	32.6	33.1	35.3	35.1	35.1	35.7	35.7	35.7	
Vent Station Steam Pressure	Bar	5.34	5.35	5.37	5.34	5.35	5.38	5.34	5.35	5.33	
In-Line Steam PCV Opening	%	100.3	100.1	100.3	100	99.9	100	94.3	94.7	89.3	
Lead Vent Station PCV Opening	%	27.4	27.6	12.1	26.5	28.2	12.4	27	27.2	15.5	
Main Steam Flow	T/H	-	-	-	266.6	266.2	269.9	289.3	284.6	285.4	
Main Steam Temperature (Scrubber Inlet)	°C	157.9	152.5	158.2	156.9	156.7	157.1	-	-	-	
Main Steam Pressure (Scrubber Inlet)	Bar	4.8	4.8	4.8	4.8	4.8	4.9	-	-	-	
Steam Scrubber Level	mm	803.4	806.3	833.4	151.9	142.3	131.3	63.2	62	53.5	
Main Steam Temperature (Turbine Inlet; LH)	°C	152.6	152.3	152.8	157.4	157.3	157.6	157.6	157.6	157.8	
Main Steam Temperature (Turbine Inlet; RH)	°C	157	156.9	157.2	157.8	157.8	158.1	157	157	157.2	
Main Steam Pressure (Turbine Inlet; LH)	Bar	5	5	5	5.1	5.1	5.2	5	5	5.1	
Main Steam Pressure (Turbine Inlet; RH)	Bar	5	5	5	5	5	5	5	5	5.1	
Blade Wash Pump Discharge Flow	T/H	6.2	6.2	6.1	-	-	-	0.8	0.8	1.1	
Main Steam Conductivity	µMHO	10.6	10.6	10.8	0	1.4	1.6	691.4	683.8	700.8	
Condenser Vacuum Pressure	Bar (a)	0.142	0.147	0.148	0.165	0.172	0.176	0.146	0.147	0.15	
Auxiliary Steam Flow	T/H	-	-	-	-	-	-	-	-	17	
Ejector Steam Supply Header Pressure	Bar	5.1	5.1	5.2	5.1	5.2	5.2	5.2	5.2	5.3	
Turbine Gland Steam Pressure	Bar	0.21	0.23	0.22	0.22	0.22	0.22	0.22	0.22	0.22	
Turbine Gland Steam PCV Opening	%	54.9	54.5	54.5	54.8	54.7	54.6	38.6	38.6	38.7	
Lube Oil Pressure (Oil Cooler Outlet)	Bar	1.55	1.55	1.54	1.72	1.7	1.7	1.54	1.53	1.52	
Main Oil Tank Level	mm	-126.8	-126	126.1	-49.9	-50.9	-40.7	-122.8	-119.1	120.8	
M.O.T. Oil Temperature	°C	66.2	66.8	66.9	66.5	67.1	67.5	63.5	63.8	64.3	
Oil Cooler Outlet Oil Temperature	°C	52.3	53.1	52.9	53.3	53.9	54.2	51.6	51.9	52.2	
Control Oil Pressure	Bar	9.4	9.4	9.4	9.5	9.5	9.5	9.2	9.2	9.2	
E/H Converter (RH) Pressure	Bar	3.1	3.05	3.23	3.27	3.25	3.28	2.31	2.33	2.33	
E/H Converter (LH) Pressure	Bar	3.32	3.26	3.27	2.63	2.55	2.69	1.83	1.86	1.84	
#1 Bearing Metal Temperature	°C	80.3	80.8	80.8	78.8	78.9	79	76.8	77.2	77.4	
Thrust Bearing Metal Temperature (GOV Side)	°C	73.7	74.1	74.1	67.5	67.7	68	68.2	68.7	68.9	
Thrust Bearing Metal Temperature (GEN Side)	°C	56.4	56.9	56.8	57.8	58.2	58.4	59.9	60.3	60.7	
#2 Bearing Metal Temperature	°C	70	70.4	70.4	66.7	67	67.1	71.4	72.1	72.3	
#3 Bearing Metal Temperature	°C	71.8	72.1	72	67.9	68.3	68.4	68.5	69	69.1	
#4 Bearing Metal Temperature	°C	64.1	64.6	64.7	71.3	71.5	71.7	78.8	79.2	79.4	
#1 Bearing Vibration (X / Y)	µm	18/17	18/18	18/18	21/-	22/-	22/-	13/15	14/15	13/15	
#2 Bearing Vibration (X / Y)	µm	24/18	23/18	24/18	-/21	-/21	-/23	14/10	14/10	14/10	
#3 Bearing Vibration (X / Y)	µm	24/17	24/16	24/16	37/19	35/19	36/19	17/12	17/12	17/12	
#4 Bearing Vibration (X / Y)	µm	19/30	19/29	20/30	-/48	-/48	-/48	5/7	5/7	5/7	
Turbine Rotor Position	mm	-0.4	-0.4	-0.4	0.1	0.1	0.1	-0.2	-0.2	-0.2	
Turbine Differential Expansion	mm	2.33	2.32	2.31	0.74	0.74	0.71	1.64	1.66	1.65	
Turbine Eccentricity (During Turning)	µm	-	-	-	-	-	-	-	-	-	
Governing Valve (LH) Opening	%	97.2	97.2	97.2	80.2	80.2	80.1	37	38.7	38	
Governing Valve (RH) Opening	%	99.9	99.9	99.9	96.2	96.2	96.2	58.3	59.9	59.5	
Turbine Steam Chest Pressure	Bar g	4.899	4.904	4.963	4.784	4.762	4.822	4.235	4.251	4.293	
Turbine Exhaust Steam Pressure	Bar a	0.141	0.145	0.148	0.165	0.171	0.174	0.142	0.146	0.15	
Turbine Exhaust Steam Temperature	°C	53	53.8	53.9	55.1	55.7	56.2	53.2	53.3	53.9	
Condenser Level	Mm	1449	1483.8	1562.4	1544.3	1667.5	1504.8	989	951	1003	
Hotwell Water Temperature	°C	50.8	51.3	51.7	50.9	51.9	51.9	52.4	53	53.1	
Circulating Water FV (Gas Cooler)	%	35.3	35.3	35.3	35.2	35.2	35.2	35.8	34.8	34.6	
Circulating Water FV (Condenser)	%	61.9	61.9	61.9	63.4	63.4	63.5	55.8	57.2	57.1	
Hotwell Pump #1 Vibration (X / Y)	mm/sec	2.1/4.1	1.8/3.8	2.1/4.0	3.7/2.6	3.1/2.1	3.1/2.1	2.5/2.5	2.5/2.3	3.1/3.9	
Hotwell Pump #1 Stator Winding Temperature	°C	-	-	-	137.7	143.7	144.3	86.9	93	91.9	
Hotwell Pump #1 Motor Inboard Brg. Metal Temp	°C	49.9	53.5	54.5	51.8	57	57.4	36.5	40.8	40.6	
Hotwell Pump #1 Motor Outboard Brg. Metal Temp	°C	65.5	69.3	71	71.8	77.6	78.9	54.3	58.1	58.2	
Hotwell Pump #1 Discharge Valve Opening	%	63.9	66.4	63.2	69.1	69.8	68.9	50	55.4	55.2	
Hotwell Pump #2 Vibration (X / Y)	mm/sec	2.8/2.4	2.7/2.8	2.4/2.4	2.8/2.5	2.7/2.4	2.7/2.6	5.9/3.5	5.4/3.6	5.9/3.5	
Hotwell Pump #2 Stator Winding Temperature	°C	133.1	136.6	137.4	146.7	149.4	150.1	95.4	97.3	97.2	
Hotwell Pump #2 Motor Inboard Brg. Metal Temp	°C	50.1	52.9	53.7	51.7	54.4	54.3	39.7	41.2	41.5	
Hotwell Pump #2 Motor Outboard Brg. Metal Temp	°C	68.5	71.9	72.4	72.7	75.7	76.3	70.3	70.1	71.2	
Hotwell Pump #2 Discharge Valve Opening	%	66.8	69.2	65.9	66.8	66.8	66.8	66.2	66.2	66.2	
Hotwell Discharge Header Pressure	Bar	1.7	1.7	1.7	1.8	1.8	1.8	1.7	1.7	1.7	
Hotwell Discharge Header Temperature	°C	50.8	51.7	51.8	53.7	54.3	54.5	52.1	52.7	53.3	
CT to Condenser Water Flow	T/H	1355.4	1459.6	1403.3	1740	1633	1925	-	-	-	
CT to Condenser Water Temp	°C	18.9	19.4	19.3	34.4	35	35.2	31.2	32	32.3	

FIGURE 1: Current parameters log sheet for 30th July 2019, page 1

		UNIT-1			UNIT-2			UNIT-3			
ITEM DESCRIPTION	**UNITS**	**800**	**1200**	**1600**	**800**	**1200**	**1600**	**800**	**1200**	**1600**	REMARKS
CT Basin Upstream Water Level	Mm	711.5	787.4	706.5	793.5	846.3	791.7	740.9	782.8	768.2	
CT Basin Downstream Water Level	Mm	624.8	701.9	610.3	679.4	757.3	674.1	613	657.7	639	
CT Fan #1 Motor Winding Temp.	°C	64.3	68.4	67	63.6	68.2	65.8	67.6	71.4	70.9	
CT Fan #2 Motor Winding Temp.	°C	62.1	66.6	64.9	97.3	98.4	100	77.9	80.9	80.8	
CT Fan #3 Motor Winding Temp.	°C	65.6	70	68.3	59.2	63	61.2	65.9	68.8	68.6	
CT Fan #4 Motor Winding Temp.	°C	63	67.7	65.7	65.4	69.7	68.4	72.1	75.6	75	
CT Fan #1 Gearbox Vibration	mm/sec	-	-	-	-	-	-	9.4	9.2	9.1	
CT Fan #2 Gearbox Vibration	mm/sec	-	-	-	-	-	-	11.5	10.5	10.3	
CT Fan #3 Gearbox Vibration	mm/sec	-	-	-	-	-	-	8.2	8.2	7.5	
CT Fan #4 Gearbox Vibration	mm/sec	-	-	-	-	-	-	10.5	10.2	10.4	
Condensate Reinjection Pump Disch. Header Press	Bar	9.3	1.9	1.9	9.6	7.9	6.2	9.4	8	1.7	
Condensate Reinjection Pump Discharge Flow	T/H	39.4	13.5	13.5	55.2	54.4	55.2	83.3	89.6	31.3	
Condensate Reinjection Pump Discharge pH	pH	1.3	1.3	1.3	-	-	-	-	-	-	
Inter-condenser Inlet Gas Header Temperature	°C	46.8	47.8	47.8	45.2	46	45.6	44.4	45.1	45.6	
Inter-condenser Inlet Gas Header Pressure	mbar	117.1	129.1	125.1	130	136.2	128.2	97.4	103.2	106.8	
Inter-condenser (A) Inner Pressure	mbar	247.7	249.1	250.3	232.4	237.8	233.2	207.4	215.1	222.1	
Inter-condenser (B) Inner Pressure	mbar	227	226.8	231.9	328.6	331.2	327.3	209	215.9	220.5	
Inter-condenser (C) Inner Pressure	mbar	228.8	231	233.5	298.8	305	308.2	515.1	528.5	520.9	
After-condenser Inner Pressure	mbar	-5.1	-5.7	-7.8	22.9	28.8	20.8	-32.8	-30.5	-32.3	
Inter-condenser (A) Outlet Temperature	°C	29.8	31.2	31.4	42.9	43.8	44	49.8	51.1	51.3	
Inter-condenser (B) Outlet Temperature	°C	46.8	47.8	47.5	52.5	52.9	53.5	51.6	52.7	53.2	
Inter-condenser (C) Outlet Temperature	°C	45.4	46.2	46.4	34.8	35.4	35.7	26.5	27.8	29.1	
After-condenser Outlet Temperature	°C	55.5	56.2	56.5	56.7	57.2	57.4	27.7	29	30.3	
Inter-condenser Outlet Pressure	mbar	224.1	226.1	225.9	318.8	322.1	319.6	204.9	211	215.1	
Inter-condenser Outlet Temperature	°C	47.7	48.5	48.7	51.3	51.8	52.2	45.9	47.1	47.6	
Vacuum Pump Motor Inboard Brg. Metal Temp.	°C	43.2	47.3	46.4	19.3	23.7	23.3	30	33.5	32.5	
Vacuum Pump Motor Outboard Brg. Metal Temp.	°C	38.4	42.6	41.4	21	24	25.3	43.2	46.9	45.8	
Vacuum Pump Inboard Brg. Metal Temp.	°C	37.8	35	35.4	21.1	23.9	23.2	28.8	31.5	31.3	
Vacuum Pump Outboard Brg. Metal Temp.	°C	38.2	39	40.8	24.8	2	27.1	34.1	35.8	35.8	
Vacuum Pump Motor Stator Winding Temp.	°C	45.9	49.5	48.3	18.3	23.2	25.2	63.8	67.1	66	
Vacuum Pump/After-condenser Outlet Temperature	°C	53	53.7	53.2	55.6	59.1	59.6	57.4	52.9	53.7	
CCWP Discharge Header Pressure	Bar g	2.5	2.5	2.4	2.6	2.6	2.6	2.56	2.56	2.55	
CCWP Discharge Strainer Diff. Pressure	Bar g	0.176	0.184	0.183	0.194	0.191	0.194	0.114	0.116	0.116	
CCW Flow to Cooling Tower	T/H	234.4	233.4	233.4	384.6	383.4	381.7	267.8	266	267.8	
CCW Flow to Inter/After-condenser etc.	T/H	-4.9	465	408.8	720.2	711.4	712.9	346.8	345.8	346.8	
CCW Discharge Temperature to Cooling Tower	°C	33.2	33.9	33.9	36.1	36.5	36.7	33.6	34.3	34.7	
CCW pH	PH	4.3	4.4	4.4	4.4	4.6	4.6	9.5	9.5	9.5	
Instrument Air Receiver Tank Pressure	Bar	7	6.7	6.9	7	6.7	7	6.7	6.9	6.8	
R2 - Brine Flow	T/H	-	-	-							
R3 – Brine Flow	T/H	-	-	-							
OW 703 – Brine Flow	T/H	-	-	-							
OW 708 Brine - Flow	T/H	-	-	-							
REMARKS:											

FIGURE 2: Current parameters log sheet for 30th July 2019, page 2

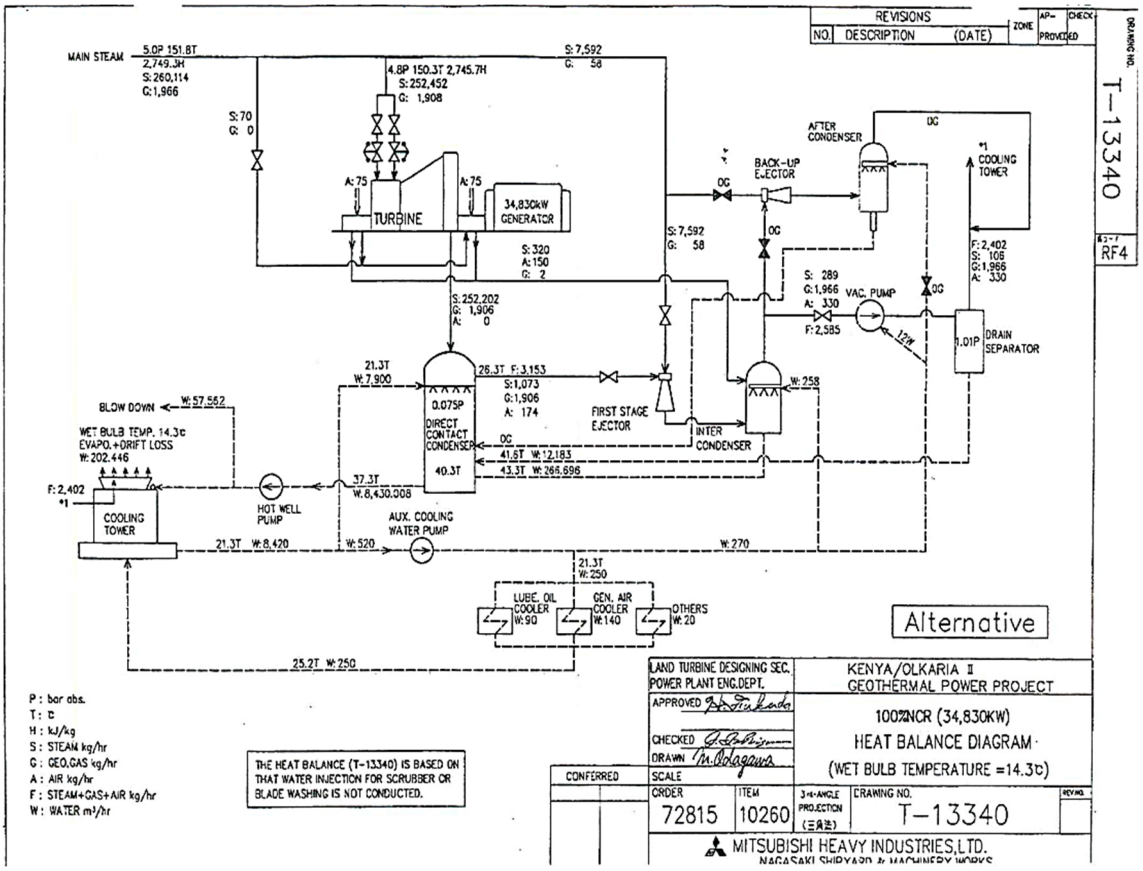

FIGURE 3: Heat mass balance diagram, units 1 and 2

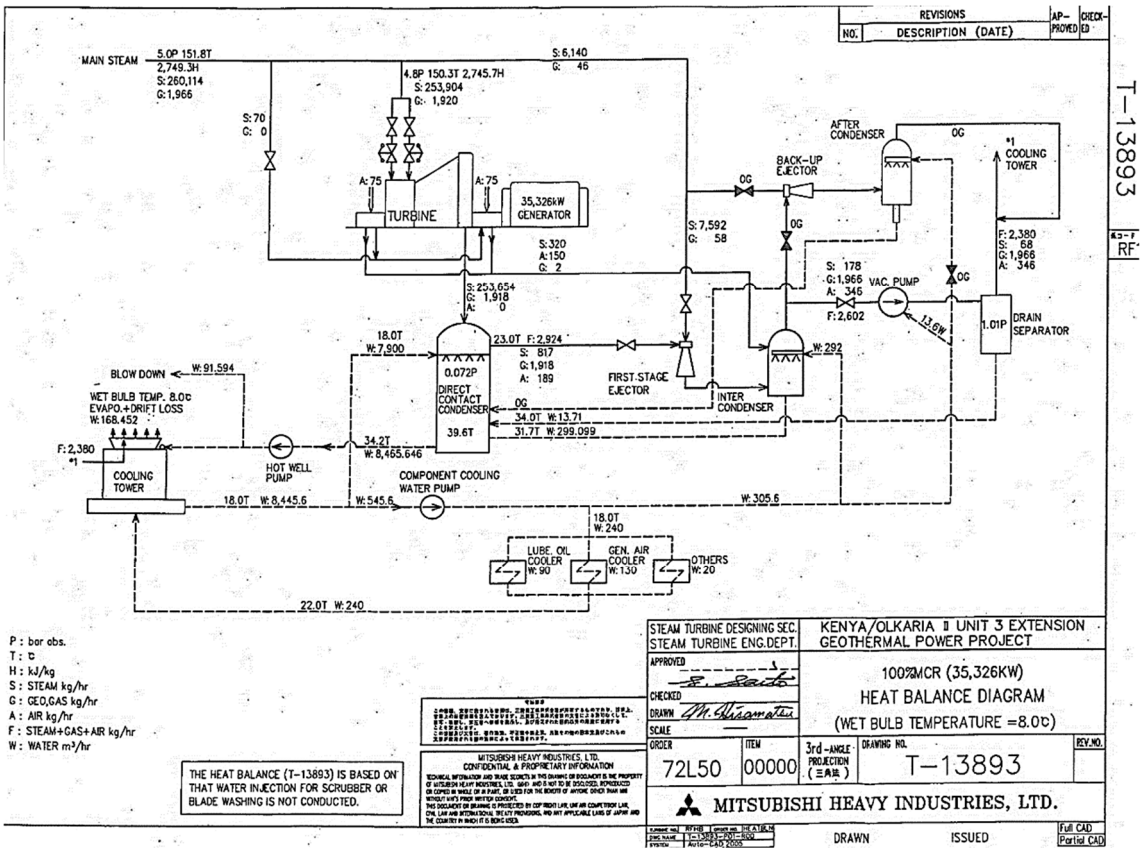

FIGURE 4: Heat mass balance diagram, unit 3

APPENDIX II: EES code design conditions for Olkaria II unit 3

{Design conditions of Olkaria II unit 3 after steam seperation}

{++}

{Code}

h[1] = **enthalpy**(***Water***; ***P***=P[1]; ***x***=1)
s[1] = **entropy**(***Water***; ***P***=P[1]; ***x***=1)
T[1] = **temperature**(***Water***; ***P***=P[1]; ***x***=1)

P[2] = P[1]
h[2] = h[1]
s[2] = **entropy**(***Water***; ***P***=P[2]; ***h***=h[2])
T[2] = **temperature**(***Water***; ***P***=P[2]; ***h***=h[2])

h_3_s = **enthalpy**(***Water***; ***P***=P[3]; ***s***=s[2])
s_3_s = s[2]
eta_isentropic = (h[2] - h[3]) / (h[2] - h_3_s)
s[3] = **entropy**(***Water***; ***P***=P[3]; ***h***=h[3])
T[3] = **temperature**(***Water***; ***P***=P[3]; ***h***=h[3])

P[4] = **pressure**(***Water***; ***T***=T[4]; ***x***=0)
s[4] = **entropy**(***Water***; ***T***=T[4]; ***x***=0)
h[4] = **enthalpy**(***Water***; ***T***=T[4]; ***x***=0)

h[5] = **enthalpy**(***Water***;***T***=T[5];***x***=0)
P[5]=**pressure**(***Water***;***T***=T[5];***x***=0)

wb[6]=**wetbulb**(***AirH2O***;***T***=T_air[6];***R***=rh[6];***P***=P1)
h_air[6]=**enthalpy**(***AirH2O***;***T***=T_air[6];***R***=rh[6];***P***=P1)
omega[6]=**humrat**(***AirH2O***;***T***=T_air[6];***R***=rh[6];***P***=P1)

wb[7]=**wetbulb**(***AirH2O***;***T***=T_air[7];***R***=rh[7];***P***=P1)
h_air[7]=**enthalpy**(***AirH2O***;***T***=T_air[7];***R***=rh[7];***P***=P1)
omega[7]=**humrat**(***AirH2O***;***T***=T_air[7];***R***=rh[7];***P***=P1)
v_air[7]=**volume**(***AirH2O***;***T***=T_air[7];***R***=rh[7];***P***=P1)
eta_coolingtower = ((T[4] - T[5])/(T[4] - wb[6]))

V_dot_air[7] = v_air[7] * m_dot_air[7]

m_dot[3]= m_dot[1]

m_dot[4] = m_dot[3] + m_dot[5]

m_dot[4] = ((h[3]*m_dot[3])+(h[5]*m_dot[5]))/h[4] {Conservation of mass and energy for a mixing fluids - condenser}

m_dot_vapour[6] = m_dot_air[6]*omega[6]

m_dot_vapour[7] = m_dot_air[7]*omega[7]

m_dot_air[6] = ((m_dot[5] * h[5])-(m_dot[4] * h[4])) / (h_air[6] - h_air[7])

m_dot_air[6] = m_dot_air[7]

m_dot_evaporation[7] = m_dot_vapour[7] - m_dot_vapour[6]

W_dot_turb = m_dot[1]* (h[2] - h[3])

Q_dot[3] = m_dot[5] * (T[4] - T[5]) * 4,186 {Heat load on the condenser = Heat Extracted by the cooling water entering the condenser}

APPENDIX III: Efficiency and heat load calculations

Sample calculations of the Olkaria II condenser heat load and cooling tower efficiency using the unit 3 design conditions. They are represented in the EES analysis models.

Input parameters:

Circulating cooling water at the inlet of cooling tower	$T_4 = 37.3℃$
Circulating cooling water at the outlet of cooling tower	$T_5 = 21.3℃$
Wet bulb temperature (WBT)	$T_{wb} = 14.3℃$
Mass flow of cooling water to the condenser from CT	$\dot{m} = 2{,}206$ kg/s
Specific heat of water	$C_p = 4.186$ kJ/kg℃

i) To find the range:

$$= T_4 - T_5$$
$$= 37.3℃ - 21.3℃$$
$$= 16℃$$

ii) To find the approach:

$$= T_5 - T_{wb}$$
$$= 21.3℃ - 14.3℃$$
$$= 7℃$$

iii) Effectiveness of the cooling tower (cooling tower efficiency, $\eta_{coolingtower}$):

$$= \frac{Range}{Range + Approach} \times 100$$
$$= \frac{16}{16 + 7} \times 100$$
$$= 69.56\ \%$$

iv) Heat load on the condenser Q_3:

$$= \dot{m} C_p (T_4 - T_5)$$
$$= 2206\ kg/s \times 4.186\ kJ/kg℃ \times (37.3℃ - 21.3℃)$$
$$= 147{,}749.056\ kJ/kg$$